Comparison of Deterministic and Stochastic Models of the *lac* Operon Genetic Network

Michail Stamatakis* and Nikos V. Mantzaris
Department of Chemical and Biomolecular Engineering, Rice University, Houston, Texas 77005

ABSTRACT The *lac* operon has been a paradigm for genetic regulation with positive feedback, and several modeling studies have described its dynamics at various levels of detail. However, it has not yet been analyzed how stochasticity can enrich the system's behavior, creating effects that are not observed in the deterministic case. To address this problem we use a comparative approach. We develop a reaction network for the dynamics of the *lac* operon genetic switch and derive corresponding deterministic and stochastic models that incorporate biological details. We then analyze the effects of key biomolecular mechanisms, such as promoter strength and binding affinities, on the behavior of the models. No assumptions or approximations are made when building the models other than those utilized in the reaction network. Thus, we are able to carry out a meaningful comparison between the predictions of the two models to demonstrate genuine effects of stochasticity. Such a comparison reveals that in the presence of stochasticity, certain biomolecular mechanisms can profoundly influence the region where the system exhibits bistability, a key characteristic of the *lac* operon dynamics. For these cases, the temporal asymptotic behavior of the deterministic model remains unchanged, indicating a role of stochasticity in modulating the behavior of the system.

INTRODUCTION

The *lac* operon genetic switch is a paradigm for genetic regulation with positive feedback, and has been studied experimentally and theoretically for nearly half a century. Indeed, the operon concept, which pertains to a sequence of genes that function under the control of the same operator (1), was first introduced in 1960. The *lac* operon consists of three genes downstream of the *lac* promoter that encode for the proteins necessary for lactose metabolism. Specifically, *lacZ* encodes for β-galactosidase, which transforms lactose to the inducer allolactose; *lacY* encodes for LacY permease, which transports lactose into the cell; and *lacA* encodes for galactoside transacetylase (LacA), which transfers an acetyl group from acetyl-CoA to β-galactosides (2). Furthermore, upstream of the promoter, there exists the constitutively expressed *lacI* gene, which encodes for the LacI repressor protein.

The free LacI repressor is a tethered tetramer (dimer of dimers) (3) that has a high affinity for the *lacO* (*O1*) operator contained in the *lac* promoter. Therefore, in the absence of lactose, each LacI dimer binds to an operator and thus inhibits transcription of the *lacZ*, *lacY*, and *lacA* genes. LacI can also bind to pseudooperators that exist upstream (*O3*) and downstream (*O2*) of the promoter and create DNA loop structures (4–6). It has been suggested that binding of the LacI repressor to the pseudooperators results in a localization of LacI close to the main operator, thereby increasing its binding efficiency to the operator (7). Thus, more efficient suppression of the *lac* genes is attained.

Submitted February 28, 2008, and accepted for publication October 29, 2008.

*Correspondence: mstam@rice.edu

Editor: Arthur Sherman.

0006-3495/09/02/0887/20 $2.00

However, if lactose is present in the extracellular medium, it gets transported into the cell, where one fraction is hydrolyzed to galactose and glucose and the other fraction is transformed to the inducer allolactose by β-galactosidase. The allolactose binds to the LacI repressor and forms a complex with reduced binding affinity to the operator. This process results in freeing the operator site(s). Induction of the LacI can also be achieved with a gratuitous inducer such as isopropyl-β-D-thiogalactopyranoside (IPTG), which does not require transformation by β-galactosidase. Instead, it can readily bind to the repressor with a stoichiometry of two IPTG molecules per LacI dimer (6).

Yet, for transcription of the *lac* operon genes to be initiated, the activator cAMP-CRP complex needs to bind to a sequence near the *lac* promoter, thereby enhancing the binding affinity of the RNA polymerase (8). High activator concentrations are brought about by low glucose concentrations. Hence, the *lac* operon genes are expressed only if the glucose concentration is low and simultaneously the lactose concentration is high. Therefore, glucose inhibits lactose metabolism in a dual manner: by reducing cAMP, and thus cAMP-CRP activator concentrations (catabolite repression); and by reducing inducer-allolactose concentrations, since it suppresses the *lac* operon genes (inducer exclusion).

Furthermore, since LacY facilitates lactose import, resulting in repressor inactivation, it follows that initial expression of the *lac* operon genes promotes further expression in an autocatalytic manner due to a positive feedback loop generated by the action of the permease. This positive genetic architecture is the cause of the experimentally observed all-or-none bistable response of the *lac* operon (9).

To reveal the role of the *lac* operon components, several experimental studies have introduced mutations to the promoter region or the coding sequences. Such mutations

doi: 10.1016/j.bpj.2008.10.028

Kinetics of Genetic Switching into the State of Bacterial Competence

Madeleine Leisner,[†‡] Jan-Timm Kuhr,[§] Joachim O. Rädler,[‡] Erwin Frey,[§] and Berenike Maier[†*]
[†]Institut für Allgemeine Zoologie und Genetik, Westfälische Wilhelms Universität, Münster, Germany; [‡]Department für Physik, Ludwig-Maximilians-Universität München, München, Germany; and [§]Arnold Sommerfeld Center for Theoretical Physics and Center for NanoScience, Department für Physik, Ludwig-Maximilians-Universität München, München, Germany

ABSTRACT Nonlinear amplification of gene expression of master regulators is essential for cellular differentiation. Here we investigated determinants that control the kinetics of the genetic switching process from the vegetative state (B-state) to the competent state (K-state) of *Bacillus subtilis*, explicitly including the switching window which controls the probability for competence initiation in a cell population. For individual cells, we found that after initiation of switching, the levels of the master regulator [ComK](t) increased with sigmoid shape and saturation occurred at two distinct levels of [ComK]. We analyzed the switching kinetics into the state with highest [ComK] and found saturation after a switching period of length 1.4 ± 0.3 h. The duration of the switching period was robust against variations in the gene regulatory network of the master regulator, whereas the saturation levels showed large variations between individual isogenic cells. We developed a nonlinear dynamics model, taking into account low-number stochastic effects. The model quantitatively describes the probability and timescale of switching at the single cell level and explains why the ComK level in the K-state is highly sensitive to extrinsic parameter variations. Furthermore, the model predicts a transition from stochastic to deterministic switching at increased production rates of ComK in agreement with experimental data.

INTRODUCTION

Populations of genetically identical cells often maintain a diversity of phenotypes, characterized by different patterns of gene expression. This is usually triggered by stochastic fluctuations, which are amplified by the underlying gene regulatory networks (1–4). The benefits of such non-genotype-derived heterogeneity lie in the enhanced adaptability to environmental changes of the population as a whole (5–8). To analyze phenotypic heterogeneity it is necessary to monitor gene expression in individual cells (9). Real-time kinetics of gene expression have been extensively measured in individual cells to characterize noise in gene expression (10–14), multistability (1,5,15,16), oscillations (16–19), and timing of gene activities (20), but the determinants for genetic switching kinetics are not well characterized so far.

Competence development in *Bacillus subtilis* is one example in which a genetic switch determines cell fate. At low cell density, a homogeneous cell population undergoes exponential growth, but at high cell density (stationary growth phase), the cell population becomes heterogeneous in its phenotype, with a well-defined fraction of 15% expressing genes that code for a strong DNA import machine and recombination proteins (21). These cells are called competent for DNA transformation and they express the master regulator *comK* at high level (22–24). In this study, the state in which *comK* expression levels are high is denoted the K-state. The entry into the K-state is switchlike (25,26). The positive feedback loop in the genetic control circuit is important for the establishment of the competent phenotype in *Bacillus subtilis* (27,28). In noncompetent cells, the positive autoregulatory loop is not activated and *comK* expression is low (B-state). During exponential growth, ComK is kept at a basal level through degradation by the MecA/ClpC/ClpP protease complex, and by transcriptional repressors including Rok, AbrB, and CodY (Fig. 1). Due to a quorum-sensing mechanism, the concentration of ComS (an inhibitor of MecA/ClpC/ClpP) rises with increasing cell density. Work by Maamar et al. (29) revealed that at T_0 (i.e., at the entry into stationary phase, $T_x=x$ h after transition point) the average number of mRNA coding for ComK per cell is of order 1. In this regime, small number fluctuations are, relative to the mean, of paramount importance. This is especially noteworthy since the reaction kinetics of ComK is highly nonlinear. Experiments and simulation have shown that the fraction of cells that switch into the K-state is determined by the magnitude of intrinsic fluctuations in *comK* expression (16,29). The second important determinant of the fraction of cells in the K-state is the length of a switching window in which basal *comK* expression rate is enhanced, which facilitates switching (30). Under conditions in which nutrient concentrations are constantly low, cycles of competence initiation and decay have been observed in real-time experiments in individual cells and a mathematical model described the system as an excitable regulatory circuit (15,16). Escape from the K-state has been attributed to negative feedback between ComK and the inhibitor of ComK proteolysis, ComS. Theoretical models of the competence decision system can be divided into two different categories, by the description of the system as excitable (15,16,31) as opposed to bistable (5,27–29,32).

Submitted May 9, 2008, and accepted for publication October 15, 2008.

*Correspondence: maierb@uni-muenster.de

Editor: Herbert Levine.

0006-3495/09/02/1178/11 $2.00

doi: 10.1016/j.bpj.2008.10.034

Leading Edge
Review

Cell

mRNA Localization: Gene Expression in the Spatial Dimension

Kelsey C. Martin[1,*] and Anne Ephrussi[2,*]
[1]Department of Psychiatry and Biobehavioral Sciences, Department of Biological Chemistry, Semel Institute for Neuroscience and Human Behavior, University of California, Los Angeles, CA 90095-1737, USA
[2]Developmental Biology Unit, European Molecular Biology Laboratory, Heidelberg D-69117, Germany
*Correspondence: kcmartin@mednet.ucla.edu (K.C.M.), ephrussi@embl.de (A.E.)
DOI 10.1016/j.cell.2009.01.044

The localization of mRNAs to subcellular compartments provides a mechanism for regulating gene expression with exquisite temporal and spatial control. Recent studies suggest that a large fraction of mRNAs localize to distinct cytoplasmic domains. In this Review, we focus on *cis*-acting RNA localization elements, RNA-binding proteins, and the assembly of mRNAs into granules that are transported by molecular motors along cytoskeletal elements to their final destination in the cell.

Introduction

The process of mRNA localization and regulated translation has classically been considered to be a mechanism used by a handful of transcripts to spatially and temporally restrict gene expression to discrete sites within highly polarized, asymmetric cells. To date, the best-studied examples of mRNA localization all involve transcripts whose protein products play specialized roles within well-defined subcellular compartments (Figure 1). These include the mRNA encoding the transcriptional repressor ASH1 in budding yeast, which inhibits mating type switching. *ASH1* mRNA is transported to the bud tip of a dividing cell such that it is delivered only to the nucleus of the daughter cell, thereby ensuring that the mother and daughter cells have distinct mating types (Paquin and Chartrand, 2008). In the fruit fly *Drosophila*, the localization of mRNAs, such as *bicoid*, *oskar*, and *nanos*, to anterior and posterior poles of the oocyte helps to establish morphogen gradients that underlie the proper spatial patterning of the developing embryo (Johnstone and Lasko, 2001). Similar processes occur in oocytes of the frog *Xenopus*, where the mRNA encoding the T-box transcription factor VegT localizes to the vegetal pole and induces endodermal and mesodermal cell fates in the embryo (King et al., 2005). In fibroblasts, *β-actin* mRNA localizes to the lamellipodia, where its translation is required for cytoskeletal-mediated motility (Condeelis and Singer, 2005). In oligodendrocytes, the mRNA encoding myelin basic protein (MBP) is transported into the distal processes where myelination occurs (Smith, 2004). During brain development, local translation of mRNAs in axonal growth cones allows neurons to respond to local environmental cues as the distal axonal processes navigate toward their synaptic partners (Lin and Holt, 2007). In the mature brain, the regulated translation of synaptically localized mRNAs allows each of the thousands of synapses made by a given neuron to autonomously alter its structure and function during synaptic plasticity, thereby greatly enhancing the computational capacity of the brain (Martin and Zukin, 2006).

Although these examples are of RNAs encoding proteins with specialized local functions, more recent studies indicate that the localization of mRNAs to particular subcellular compartments may be much more prevalent than previously thought. In a recent study involving high-throughput, high-resolution in situ hybridizations of over 3000 transcripts in *Drosophila* embryos, 71% were found to be expressed in spatially distinct patterns (Lecuyer et al., 2007) (Figure 2). Similarly, in mammalian neurons, it was once thought that only a handful of mRNAs localized at synapses. However, more recent studies indicate that hundreds of mRNAs are present in neuronal processes, where they encode diverse functionalities (Eberwine et al., 2002; Martin and Zukin, 2006). Further, the analysis of RNA localization in migrating fibroblasts (Mili et al., 2008), *Xenopus* oocytes (Blower et al., 2007), and *Drosophila* embryos (Lecuyer et al., 2007) may reveal subcellular compartments that had previously been unappreciated, and thus these findings may lead to a more detailed and nuanced understanding of cellular architecture.

What are the advantages of regulating gene expression by mRNA localization? The most obvious is that it allows gene expression to be spatially restricted within the cytoplasm. A second advantage is that this spatially restricted gene expression can be achieved with high temporal resolution given that local stimuli can regulate translation on-site instead of requiring a signal to be delivered to the nucleus to initiate transcription, followed by mRNA export, cytoplasmic translation, and subsequent targeting of the protein to the site of stimulation. A third advantage is one of economy—localized mRNAs can be translated multiple times to generate many copies of a protein, which is much more efficient than translating mRNAs elsewhere in the cell, then transporting each protein individually to a distinct site. A fourth advantage, exemplified by the localization of *MBP* mRNA in oligodendrocytes, is that the local translation of proteins can protect the rest of the cell from proteins that might be toxic or deleterious in other cellular compartments.

The targeting of mRNAs to specific subcellular sites involves multiple steps. The cellular "address" of transcripts is encoded by *cis*-acting elements in the RNA. As detailed below, these *cis*-acting elements, called "localization elements" or "zipcodes," are most frequently found in the 3′ untranslated region (UTR), although in some cases they are present in the 5′UTR or in the coding sequence. Localization elements are recognized by specific RNA-binding proteins that often function both in

Cell

Old Nuclei Spring New Leaks

Chitra V. Kotwaliwale[1,2,*] and Abby F. Dernburg[1,2,3,*]
[1]Howard Hughes Medical Institute
[2]Department of Molecular and Cell Biology, University of California, Berkeley
[3]Life Sciences Division, Lawrence Berkeley National Laboratory
Berkeley, CA 94720, USA
*Correspondence: chitra.kot@gmail.com (C.V.K.), afdernburg@lbl.gov (A.F.D.)
DOI 10.1016/j.cell.2009.01.004

The nuclear pore complex (NPC) regulates the bidirectional movement of cell components across the nuclear envelope. In this issue, D'Angelo et al. (2009) demonstrate that the NPC loses essential protein subunits as cells age, resulting in increased nuclear permeability and potentially contributing to organismal aging.

The compartmentalization of genetic information within a membrane-bound organelle—the nucleus—is a defining feature of higher organisms. This strategy for cellular organization uncouples the processes of transcription and translation, enabling eukaryotes to deploy mechanisms of posttranscriptional gene regulation that are absent in prokaryotes. Trafficking of large molecules between the nucleus and cytoplasm is governed by the nuclear pore complexes (NPCs), which span the double lipid bilayer of the nuclear envelope. NPCs and their protein components (nucleoporins) have been implicated in cellular processes that appear unrelated to their primary function in transport. In particular, nucleoporins have been found to contribute to the regulation of gene expression, cell-cycle progression, maintenance of nuclear envelope integrity, and chromosome segregation (reviewed by D'Angelo and Hetzer, 2006). In light of these diverse roles, it is perhaps not surprising that nuclear pore dysfunction or mutations in nucleoporins have been associated with a number of human diseases, including certain forms of cancer and an inherited form of atrial fibrillation, a cardiac disorder that can lead to early death (Zhang et al., 2008). In this issue, provocative new work by D'Angelo et al. (2009) further expands our understanding of the NPC by uncovering a link between NPC function and the process of aging.

Nuclear pores, first reported in 1950 (Callan and Tomlin, 1950), are a ubiquitous feature of eukaryotic nuclear envelopes. These massive complexes are present in several thousand copies in vertebrate cells and allow the passive diffusion of small molecules of up to 40 kilodaltons (kDa) (Figure 1). The movement of larger molecules across the nuclear pore requires signal-mediated interactions between the molecular cargoes and transport proteins (karyopherins). Proteomic analysis has revealed that NPCs are composed of at least 30–50 different nucleoporins that assemble in an ordered fashion to form a structure with 8-fold symmetry. Some of these nucleoporins act as "scaffolds." A subset of these scaffold nucleoporins are transmembrane proteins that anchor the nuclear pores within the membrane. Peripheral nucleoporins assemble on these scaffolds to establish the permeability barrier in the pore. Whereas peripheral nucleoporins are dynamically exchanged between NPCs throughout the cell cycle, the scaffold proteins are thought to reorganize only during M phase and indeed may not fully disassemble even during mitosis. NPCs are also known to contain a subset of unusually stable proteins, as evidenced by their extremely slow turnover in mammalian cells (Daigle et al., 2001; Rabut

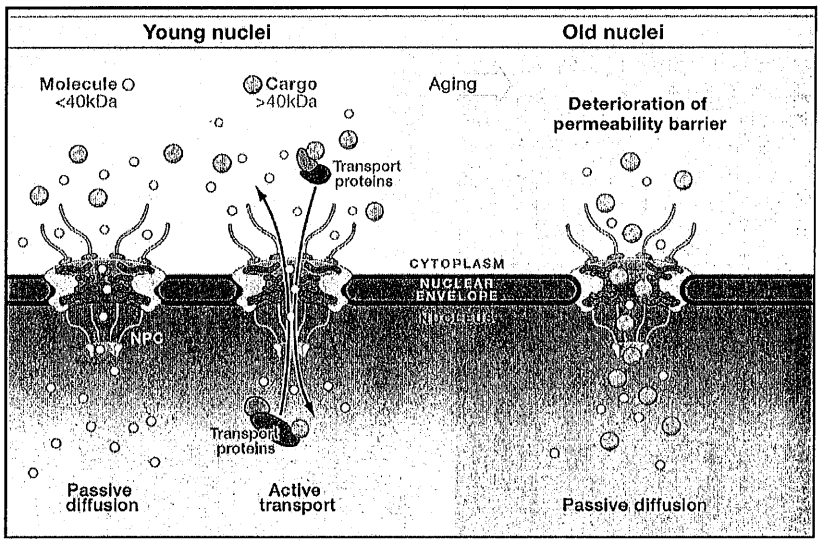

Figure 1. NPC Function Declines with Age
Nuclear pore complexes (NPCs) mediate the movement of molecules across the nuclear envelope and establish a permeability barrier. This barrier blocks the passive diffusion of molecules >40 kilodaltons (kDa) in size. To enter or exit the nucleus, these cargo molecules require association with transport proteins to pass through the nuclear pore (left). Protein subunits (nucleoporins) that constitute the scaffold of the NPC do not turn over and remain stably assembled for long periods of time in postmitotic cells. As some cells age (right), their nuclei become "leaky" and exhibit a loss of the permeability barrier. This is likely due to the selective depletion of certain nucleoporins such as Nup93 from the NPC, perhaps as a result of oxidative damage to proteins in aging cells.

Cell

The Native 3D Organization of Bacterial Polysomes

Florian Brandt,[1,2] Stephanie A. Etchells,[2] Julio O. Ortiz,[1] Adrian H. Elcock,[4] F. Ulrich Hartl,[2,3,*] and Wolfgang Baumeister[1,3,*]
[1]Department of Molecular Structural Biology
[2]Department of Cellular Biochemistry
Max Planck Institute of Biochemistry, Am Klopferspitz 18, Martinsried 82152, Germany
[3]Center for Integrated Protein Science Munich, Ludwig-Maximilians-Universität München, Butenandtstr. 5-13, München 81377, Germany
[4]Department of Biochemistry, University of Iowa, 4-530 Bowen Science Building, 51 Newton Road, Iowa City, IA 52242, USA
*Correspondence: uhartl@biochem.mpg.de (F.U.H.), baumeist@biochem.mpg.de (W.B.)
DOI 10.1016/j.cell.2008.11.016

SUMMARY

Recent advances have led to insights into the structure of the bacterial ribosome, but little is known about the 3D organization of ribosomes in the context of translating polysomes. We employed cryoelectron tomography and a template-matching approach to map 70S ribosomes in vitrified bacterial translation extracts and in lysates of active *E. coli* spheroplasts. In these preparations, polysomal arrangements were observed in which neighboring ribosomes are densely packed and exhibit preferred orientations. Analysis of characteristic examples of polysomes reveals a staggered or pseudohelical organization of ribosomes along the mRNA trace, with the transcript being sequestered on the inside, the tRNA entrance sites being accessible, and the polypeptide exit sites facing the cytosol. Modeling of elongating nascent polypeptide chains suggests that this arrangement maximizes the distance between nascent chains on adjacent ribosomes, thereby reducing the probability of intermolecular interactions that would give rise to aggregation and limit productive folding.

INTRODUCTION

Ribosomes are the essential machines of protein synthesis in all cells. Much has been learned in recent years about the structure and function of the bacterial ribosome from crystallography (Ban et al., 2000; Schuwirth et al., 2005; Wimberly et al., 2000) and single-particle analysis by cryoelectron microscopy (Agrawal et al., 2000; Gabashvili et al., 2000; Valle et al., 2003a). Significant progress has been made in understanding the pathway of the synthesized peptide through the exit tunnel of the 50S ribosomal subunit and its interactions with ribosomal components and molecular chaperones (Bashan and Yonath, 2005; Baram et al., 2005; Hsu et al., 2007). In contrast, little is known about the spatial arrangement of individual ribosomes in the context of polysomes during active protein synthesis.

Linear polysomal arrays of translating ribosomes were first observed in reticulocyte translation lysates by sedimentation analysis and conventional transmission electron microscopy (TEM) (Warner et al., 1962). Various polysome arrangements have been described from TEM micrographs of mammalian and bacterial cells (Rich, 1963; Slayter et al., 1968; Staehelin et al., 1963). More recently, wheat germ polysomes formed in vitro have been reported to adopt ordered structure (Kopeina et al., 2008; Madin et al., 2004). However, the preparation methods of metal shadowing or negative staining used previously may be prone to artifacts. In contrast, cryoelectron microscopy (cryo-EM) single-particle analysis avoids the staining and dehydration problems but requires essentially repetitive structures, a prerequisite not met by supramolecular assemblies such as polysomes. Moreover, two-dimensional TEM projections do not per se provide insight into the three-dimensional (3D) organization of molecular assemblies.

Cryoelectron tomography (CET) overcomes these limitations and allows us to obtain a 3D model of native polysomes into which the high-resolution map of the ribosome can be docked. CET is a powerful method to reconstruct the 3D electron densities of individual macromolecular objects in a close-to-native environment without the need to stain or fix the specimen (Lucic et al., 2005). A comprehensive interpretation of tomograms is achieved by pattern recognition based on crosscorrelation between a known high-resolution structure and target structures in the tomogram, as demonstrated with macromolecular complexes enclosed in phantom cells (Bohm et al., 2000; Frangakis et al., 2002). At present, however, the application of this method to intact cells is limited due to the low signal-to-noise ratio of cellular tomograms, particularly when working with prokaryotic cells exceeding 0.5 μm in thickness. Although, in thin, intact cells, CET allows the determination of coordinates and orientations of large complexes, such as 70S ribosomes, at an intermediate resolution of 4–5 nm (Ortiz et al., 2006), an unambiguous identification of individual polysome structures is hard to achieve due to the crowding of these systems. Since the analysis of polysome organization requires the reliable localization and correct identification of individual ribosomes bound to the same mRNA, we decided to work with actively translating cell lysates or *E. coli* spheroplast lysates in order to achieve

Cell

Aneuploidy Underlies Rapid Adaptive Evolution of Yeast Cells Deprived of a Conserved Cytokinesis Motor

Giulia Rancati,[1,3] Norman Pavelka,[1,3] Brian Fleharty,[1] Aaron Noll,[1] Rhonda Trimble,[1] Kendra Walton,[1] Anoja Perera,[1] Karen Staehling-Hampton,[1] Chris W. Seidel,[1] and Rong Li[1,2,*]
[1]Stowers Institute for Medical Research, 1000 E. 50th Street, Kansas City, MO 64110, USA
[2]Department of Physiology, University of Kansas Medical Center, 3901 Rainbow Boulevard, Kansas City, KS 66160, USA
[3]These authors contributed equally to this work
*Correspondence: rli@stowers-institute.org
DOI 10.1016/j.cell.2008.09.039

SUMMARY

The ability to evolve is a fundamental feature of biological systems, but the mechanisms underlying this capacity and the evolutionary dynamics of conserved core processes remain elusive. We show that yeast cells deleted of *MYO1*, encoding the only myosin II normally required for cytokinesis, rapidly evolved divergent pathways to restore growth and cytokinesis. The evolved cytokinesis phenotypes correlated with specific changes in the transcriptome. Polyploidy and aneuploidy were common genetic alterations in the best evolved strains, and aneuploidy could account for gene expression changes due directly to altered chromosome stoichiometry as well as to downstream effects. The phenotypic effect of aneuploidy could be recapitulated with increased copy numbers of specific regulatory genes in *myo1Δ* cells. These results demonstrate the evolvability of even a well-conserved process and suggest that changes in chromosome stoichiometry provide a source of heritable variation driving the emergence of adaptive phenotypes when the cell division machinery is strongly perturbed.

INTRODUCTION

Evolution is the creative force that shapes life on earth (Darwin, 1859). As such, evolvability, the ability to generate heritable variation to adjust to internal and external changes, should be a fundamental property of all living systems. It has been hypothesized that evolvability may be linked to the robustness and flexibility that characterize complex biological systems (Kirschner and Gerhart, 1998; Wagner and Altenberg, 1996). Whereas recent studies have shed light on the generation of robustness from complexity and redundancy in molecular pathways (Kitano, 2004; Wagner, 2005), it remains poorly understood how evolvability is related to these properties and, in turn, affects the dynamics of biological systems under varying physiological or pathological conditions. Experimental exploration into this relationship may bring fundamental insights into the design principles underlying biological systems and ultimately improve our ability to manipulate these systems for research and therapeutic goals.

Another important question in the understanding of cellular evolvability is the source of the heritable variation that could drive rapid phenotypic changes. At the molecular level, genetic changes can be generated through at least four different mechanisms: (1) point mutations in the nucleotide sequence of coding or noncoding regions; (2) amplification or deletion of chromosomal segments; (3) chromosomal translocation, inversion, and nonhomologous end joining; and (4) whole-chromosome aneuploidy. It is presently unclear how the different types of genetic changes may be particularly advantageous in evolutionary processes with different timescales, population sizes, and the degrees of the phenotypic leap under specific selective conditions. Another genomic change implicated in evolution is polyploidization, which is thought to facilitate evolution through increased gene dosage, the capacity to mask deleterious mutations, and elevated genomic instability (Otto, 2007).

In this study we have used cytokinesis in the budding yeast *Saccharomyces cerevisiae* as a model system to gain insights into cellular evolvability. Successful cytokinesis is accomplished through a fully integrated process of cell-cycle regulation, spatial patterning, cytoskeletal rearrangements, force production, and membrane trafficking (Balasubramanian et al., 2004; Eggert et al., 2006). In yeast and animal cells, cytokinesis relies on membrane constriction along an equatorial furrow, driven by a ring structure consisting of actin filaments, the nonmuscle myosin II, and a number of other cytoskeleton-associated proteins. In budding yeast, Myo1, the only myosin II, is required for ingression of the bud neck membrane and guides the production of a single primary septum by the transmembrane chitin synthase, Chs2 (Schmidt et al., 2002; Tolliday et al., 2003). Despite a high level of conservation, accumulating observations in yeast and other cell types suggest that the cytokinetic machinery may be highly adaptable (Kanada et al., 2005; Nagasaki et al., 2002; Schmidt et al., 2002; Tolliday et al., 2003). Here we took a systematic approach to investigate the evolvability of *myo1Δ* yeast cells. Forty-five lines of freshly isolated *myo1Δ* colonies, which

THE EMBO JOURNAL

Have you seen ...?

The EMBO Journal (2009) 28, 171–172 | © 2009 European Molecular Biology Organization | Some Rights Reserved 0261-4189/09
www.embojournal.org

RodZ, a new player in bacterial cell morphogenesis

Kenn Gerdes*

Centre for Bacterial Cell Biology, Institute for Cell and Molecular Biosciences, Newcastle University, Newcastle upon Tyne, UK
*Corresponding author. Centre for Bacterial Cell Biology, Institute for Cell and Molecular Biosciences, Newcastle University, Framlington Place, Newcastle upon Tyne NE2 4HH, UK.
E-mail: kenn.gerdes@ncl.ac.uk

The EMBO Journal (2009) **28,** 171–172. doi:10.1038/emboj.2008.287

Three different laboratories have now identified a new morphogenetic factor widely conserved in bacteria. The protein, RodZ, is required for assembly of the actin cytoskeleton MreB that controls cell wall synthesis and cell shape.

It is not yet understood how bacteria determine their shape. Almost all bacteria are surrounded by a giant cell wall polymer called peptidoglycan that gives shape to the cells and is an important target of antibiotics. Thus, one main aim is to understand the highly complex enzymatic machinery that synthesizes peptidoglycan and how its activity is coordinated with cell growth and division. The rod-shaped bacteria *Escherichia coli* and *Bacillus subtilis* and the curved *Caulobacter crescentus* have been used extensively as models in the study of cell morphogenesis. A paradigm has emerged in which the essential actin homologue MreB, discovered by Masaaki Wachi many years ago (Wachi *et al*, 1987), is a key player. In the beginning of the decade, it was shown that MreB of *B. subtilis* forms helical structures beneath the cell surface and that these structures are required to maintain cell shape (Jones *et al*, 2001). Later studies confirmed that MreBs of *E. coli* and *C. crescentus* (Kruse *et al*, 2003; Figge *et al*, 2004) played a similar role. MreB interacts with MreC and MreD and these latter proteins are also essential to cell shape maintenance (Kruse *et al*, 2005). MreB and MreC are inner membrane proteins much less abundant than MreB (Wachi *et al*, 2006). Bacterial two-hybrid analyses and pull-down experiments showed that MreC interacts with the penicillin-binding proteins that synthesize the cell wall and therefore are cell shape determinants (Divakaruni *et al*, 2005, 2007; van den Ent *et al*, 2006). These results raised the possibility that the MreB filaments interact with MreCD complexes located in the inner cell membrane and thereby control the activity of the external cell wall-synthesizing protein complexes in space and time. This conjecture was supported by the observation that MreC forms helical structures that alternate with the MreB helices (Dye *et al*, 2005). This simple model is shown schematically in Figure 1.

A new common player in bacterial cell morphogenesis has now been discovered independently by three different laboratories, published in separate issues of the *EMBO Journal* (Shiomi *et al*, 2008; Bendezu *et al*, 2009), and *Proc Natl Acad Sci USA* (Alyahya *et al*, 2009). Hironori Niki's group screened the Keio strain collection of gene deletions and thereby identified a novel gene, *rodZ* (*yfgA*) that is required to maintain proper cell shape. Cells lacking the *rodZ* gene were round or otherwise misshapen and exhibited a highly reduced growth rate. The diameters of the majority of the *rodZ*-null cells were similar to that of the width of wild-type *E. coli* cells and the Niki group therefore suggested that RodZ is a primary determinant of cell length. In that model, cell width is maintained by the MreBCD and PBP2/RodA complexes. Overproduction of RodZ resulted in an increased cell length with little or no change of cell width, consistent with the model.

Piet de Boer's group identified *rodZ* by screening for the requirement for extra FtsZ, as it was known that increased FtsZ levels rescue the lack of other cell shape determinants (i.e. MreB and PBP2) (Bendezu and de Boer, 2008). They also found that *rodZ*-null cells exhibited a cold-sensitive phenotype. At low temperatures, the cells were non-dividing large and misshapen spheres.

RodZ is a remarkable multidomain protein that, similar to MreB, forms helical structures associated with the cell membrane (Figure 1). RodZ has one single trans-membrane domain that divides the protein into a cytosolic and a periplasmic part. Interestingly, RodZ has a helix-turn-helix DNA-binding motif (λ Cro type) in its N-terminal cytosolic domain. A deletion analysis showed that the HTH motif was required for the formation of RodZ helices and for full complementation of the defective shape of *rodZ*-null cells. The function of the HTH domain is unknown but bacterial two-hybrid data indicated that it may mediate important interactions between RodZ and MreB. However, it is also possible that the HTH motif somehow links the nucleoid to the cell wall. The detailed deletion analysis by the de Boer group showed that the basic juxta-membrane (JM) domain of RodZ (marked as + + + in

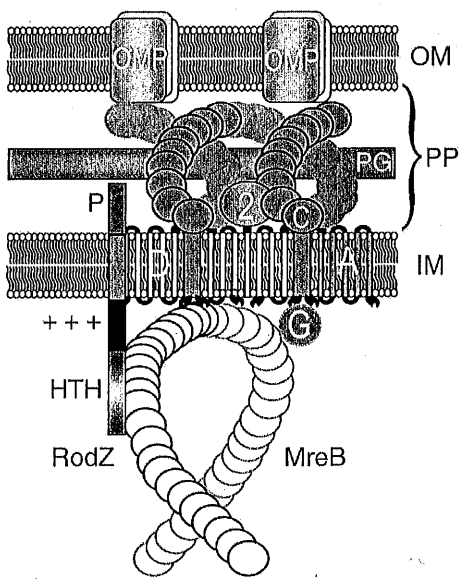

Figure 1 Schematic diagram that visualizes the interactions between RodZ and the MreBCD–MrdAB (PBP2 RodA) complexes of *E. coli*. RodZ is shown as a vertical bar with four domains. The HTH domain (magenta) mediates interaction with MreB, whereas the juxta-membrane (JM) domain (+ + +) is in close contact with the negatively charged membrane phospholipids and serves to configure MreB in its helix-like appearance. P is the periplasmic part of RodZ that interacts with as yet unknown components in the periplasm. MreB is shown as a yellow helix beneath the inside of the inner membrane (IM) that interacts with MreC (red helix). MreC, in turn, interacts with PBP2 (green) and different OMPs. PP, periplasm; OM, outer membrane; PG, peptidoglycan layer; D, MreD in the IM; A, RodA in the IM.

The EMBO Journal (2009) 28, 193–204 | © 2009 European Molecular Biology Organization | All Rights Reserved 0261-4189/09
www.embojournal.org

THE EMBO JOURNAL

RodZ (YfgA) is required for proper assembly of the MreB actin cytoskeleton and cell shape in *E. coli*

Felipe O Bendezú[1], Cynthia A Hale, Thomas G Bernhardt[2] and Piet AJ de Boer*

Department of Molecular Biology and Microbiology, School of Medicine, Case Western Reserve University, Cleveland, OH, USA

The bacterial MreB actin cytoskeleton is required for cell shape maintenance in most non-spherical organisms. In rod-shaped cells such as *Escherichia coli*, it typically assembles along the long axis in a spiral-like configuration just underneath the cytoplasmic membrane. How this configuration is controlled and how it helps dictate cell shape is unclear. In a new genetic screen for cell shape mutants, we identified RodZ (YfgA) as an important transmembrane component of the cytoskeleton. Loss of RodZ leads to misassembly of MreB into non-spiral structures, and a consequent loss of cell shape. A juxta-membrane domain of RodZ is essential to maintain rod shape, whereas other domains on either side of the membrane have critical, but partially redundant, functions. Though one of these domains resembles a DNA-binding motif, our evidence indicates that it is primarily responsible for association of RodZ with the cytoskeleton.

The EMBO Journal (2009) **28,** 193–204. doi:10.1038/emboj.2008.264; Published online 11 December 2008
Subject Categories: cell & tissue architecture; microbiology & pathogens
Keywords: MreC; MreD; PBP2; RodA; FtsZ

Introduction

Bacterial MreB actin has been implicated in cell shape maintenance, chromosome segregation and cell polarization events in a variety of rod-shaped species, including the well-studied model organisms *Bacillus subtilis*, *Caulobacter crescentus* and *Escherichia coli*. The shape of most bacterial cells is dictated by the shape of the murein (peptidoglycan) sacculus, in essence a giant and dynamic cell-shaped molecule that surrounds the entire cytoplasmic membrane. How, despite often considerable turgor pressure, non-coccal organisms manage to mould and maintain this molecule in a particular shape is an unsolved and intensely studied issue (for reviews, see Shih and Rothfield, 2006; Cabeen and Jacobs-Wagner, 2007; den Blaauwen *et al*, 2008).

The MreB protein of *E. coli* is the only known actin in the cell and, as in other species, accumulates just underneath the cytoplasmic membrane in a spiral/banded-like pattern along the long axis of the cell (Jones *et al*, 2001; van den Ent *et al*, 2001; Kruse *et al*, 2003; Shih *et al*, 2003; Figge *et al*, 2004; Gitai *et al*, 2005). Clear evidence for an important role of MreB in cell shape maintenance came from the isolation of spherical *E. coli mreB* mutants more than 20 years ago (Wachi *et al*, 1987), well before the protein was recognized as an actin. About that time the four additional proteins that are currently known to be critical in determining cell shape, MreC, MreD, penicillin-binding protein 2 (PBP2) and RodA were identified as well (Tamaki *et al*, 1980; Wachi *et al*, 1989). The genes for MreC and MreD reside with *mreB* in the *mreBCD* operon, whereas those for PBP2 (MrdA) and RodA (MrdB) reside in the unlinked *mrd* operon. Although MreB is cytoplasmic, MreC and PBP2 are bitopic and MreD and RodA are polytopic cytoplasmic membrane species. PBP2 is the only murein synthase in *E. coli* that is specifically required for extension of the cylindrical portion of the sacculus during cell elongation (Spratt, 1975; de Pedro *et al*, 2001; Vollmer and Bertsche, 2008). RodA is likely needed for proper PBP2 function (Ishino *et al*, 1986; de Pedro *et al*, 2001).

MreC forms a dimer and is thought to interact with MreB, MreD and several of the high molecular weight murein synthases (PBPs), including PBP2 (Divakaruni *et al*, 2005, 2007; Dye *et al*, 2005; Kruse *et al*, 2005; van den Ent *et al*, 2006). MreC, MreD and PBP2 accumulate in a spotty or helical manner along the cell envelope in *E. coli*, *B. subtilis* and/or *C. crescentus* (den Blaauwen *et al*, 2003; Figge *et al*, 2004; Divakaruni *et al*, 2005; Dye *et al*, 2005; Leaver and Errington, 2005). These localization patterns are reminiscent of that of MreB, as well as of the helical patterns of new murein insertion that have been observed along the cylindrical portions of rod-shaped cells. (Daniel and Errington, 2003; Tiyanont *et al*, 2006; Divakaruni *et al*, 2007; Varma *et al*, 2007). Hence, it is proposed that the helical actin fibres function as cytoplasmic tracks for murein synthase and/or hydrolase activities in the periplasm. This would topologically constrain these activities, resulting in helical insertion of new murein and elongation of the cell (Daniel and Errington, 2003; Figge *et al*, 2004; Carballido-Lopez *et al*, 2006).

The MreB cytoskeleton has also been implicated in chromosome segregation in several organisms (Kruse *et al*, 2003, 2006; Soufo and Graumann, 2003; Gitai *et al*, 2005; Srivastava *et al*, 2007). However, such a role is not evident in all bacteria (Hu *et al*, 2007), and additional studies have cast doubt on a critical role of MreB in chromosome segregation in *B. subtilis* and *E. coli* (Formstone and Errington, 2005; Karczmarek *et al*, 2007).

To help elucidate the assembly and/or functions of the MreB cytoskeleton in bacteria, we sought to identify additional proteins required for maintaining the normal rod shape

*Corresponding author. Department of Molecular Biology and Microbiology, School of Medicine, Case Western Reserve University, W213, 10900 Euclid Avenue, Cleveland, OH 44106, USA.
Tel.: +1 216 368 1697; Fax: +1 216 368 3055;
E-mail: pad5@case.edu
[1]Present address: Center for Integrative Genomics, University of Lausanne, Lausanne, Switzerland
[2]Present address: Department of Microbiology and Molecular Genetics, Harvard Medical School, Boston, MA, USA

Received: 8 November 2008; accepted: 24 November 2008; published online: 11 December 2008

A Publication of The Genetics Society of America

GENETICS

Originally published as *Genetics* Published Articles Ahead of Print on October 14, 2008.

Genetics, Vol. 180, 2193-2200, December 2008, Copyright © 2008
doi:10.1534/genetics.108.093013

Surviving the Bottleneck: Transmission Mutants and the Evolution of Microbial Populations

Andreas Handel[*],[1],[2] and Matthew R. Bennett[†],[1]

[*] Department of Biology, Emory University, Atlanta, Georgia 30322 and [†] Department of Bioengineering and Institute for Nonlinear Science, University of California, San Diego, California 92093

[2] *Corresponding author:* Department of Epidemiology and Biostatistics, University of Georgia, Athens, GA 30602 (as of January, 2009).
E-mail: andreas.handel@gmail.com

The ability of microbial populations to increase fitness through fixation of mutants with an increased growth rate has been well described. In experimental studies, this is often the only way fitness can be increased. In natural settings, however, fitness can also be improved by increasing the ability of the microbe to transmit from one host to the next. For many pathogens, transmission includes a phase outside the host during which they need to survive before the chance of reinfecting a new host occurs. In such a situation, a reduced death rate during this phase will lead to improved fitness. Here, we compute the fixation probability of mutants that better survive the transmission bottleneck during the evolution of microbial populations. We derive analytical results that show that transmission mutants are often likely to occur and that their importance relative to growth mutants increases as the population decline during the transmission phase increases. We confirm our theoretical results with numerical simulations and suggest specific experiments that can be done to test our predictions.

THIS ARTICLE
Full Text
Full Text (PDF)
All Versions of this Article:
genetics.108.093013v1
180/4/2193 *most recent*
Alert me when this article is cited
Alert me if a correction is posted

SERVICES
Email this article to a friend
Related articles in Genetics
Similar articles in this journal
Similar articles in PubMed
Alert me to new issues of the journal
Download to citation manager
Reprints & Permissions

GOOGLE SCHOLAR
Articles by Handel, A.
Articles by Bennett, M. R.

PUBMED
PubMed Citation
Articles by Handel, A.
Articles by Bennett, M. R.

Related articles in Genetics:

ISSUE HIGHLIGHTS

Genetics 2008 180: NP. [Full Text]

Online ISSN: 1943-2361 Print ISSN: 0016-6731

A Publication of The Genetics Society of America

GENETICS

Originally published as *Genetics* Published Articles Ahead of Print on October 1, 2008.

Genetics, Vol. 180, 2163-2173, December 2008, Copyright © 2008
doi:10.1534/genetics.108.090019

Clonal Interference, Multiple Mutations and Adaptation in Large Asexual Populations

Craig A. Fogle*, James L. Nagle* and Michael M. Desai†,1

* Department of Physics, University of Colorado, Boulder, Colorado 80309 and † Lewis–Sigler Institute for Integrative Genomics, Princeton University, Princeton, New Jersey 08544

1 *Corresponding author:* Lewis-Sigler Institute for Integrative Genomics, Princeton University, Princeton, NJ 08544. E-mail: mmdesai@princeton.edu

Two important problems affect the ability of asexual populations to accumulate beneficial mutations and hence to adapt. First, clonal interference causes some beneficial mutations to be outcompeted by more-fit mutations that occur in the same genetic background. Second, multiple mutations occur in some individuals, so even mutations of large effect can be outcompeted unless they occur in a good genetic background that contains other beneficial mutations. In this article, we use a Monte Carlo simulation to study how these two factors influence the adaptation of asexual populations. We find that the results depend qualitatively on the shape of the distribution of the fitness effects of possible beneficial mutations. When this distribution falls off slower than exponentially, clonal interference alone reasonably describes which mutations dominate the adaptation, although it gives a misleading picture of the evolutionary dynamics. When the distribution falls off faster than exponentially, an analysis based on multiple mutations is more appropriate. Using our simulations, we are able to explore the limits of validity of both of these approaches, and we explore the complex dynamics in the regimes where neither one is fully applicable.

THIS ARTICLE

Full Text

Full Text (PDF)

All Versions of this Article:
genetics.108.090019v1
180/4/2163 *most recent*

Alert me when this article is cited

Alert me if a correction is posted

SERVICES

Email this article to a friend

Similar articles in this journal

Similar articles in PubMed

Alert me to new issues of the journal

Download to citation manager

Reprints & Permissions

GOOGLE SCHOLAR

Articles by Fogle, C. A.

Articles by Desai, M. M.

PUBMED

PubMed Citation

Articles by Fogle, C. A.

Articles by Desai, M. M.

Online ISSN: 1943-2361 Print ISSN: 0016-6731

phone: 412-268-1812 fax: 412-268-1813 email: genetics-gsa@andrew.cmu.edu

J|A|C|S COMMUNICATIONS

Published on Web 02/06/2009

Hydrophilic Fluorescent Nanogel Thermometer for Intracellular Thermometry

Chie Gota,[†] Kohki Okabe,[†,‡] Takashi Funatsu,[†,§] Yoshie Harada,[‡] and Seiichi Uchiyama*[,†]

Graduate School of Pharmaceutical Sciences, The University of Tokyo, 7-3-1 Hongo, Bunkyo-ku, Tokyo 113-0033, Japan, The Tokyo Metropolitan Institute of Medical Science, 3-18-22, Honkomagome, Bunkyo-ku, Tokyo 113-8613, Japan, and Center for NanoBio Integration, The University of Tokyo, 7-3-1 Hongo, Bunkyo-ku, Tokyo 113-8656, Japan

Received September 30, 2008; E-mail: seiichi@mol.f.u-tokyo.ac.jp

The temperature of a living cell is changeable during every cellular event, such as cell division, gene expression, enzyme reaction, and metabolism. In 1932, for instance, significant thermogenesis was found in ATP hydrolysis,[1] underlying the present bioenergetics. In mitochondria, surplus energy in ATP production is released in the form of heat, and a consequent rise in temperature coordinates other cellular events.[2] From a clinical viewpoint, pathological cells are warmer than normal cells because of their enhanced metabolic activity.[3] Thus, measuring cellular temperature can contribute to the explanation of intricate biological processes and the development of novel diagnoses. Here we demonstrate for the first time intracellular thermometry with a newly developed fluorescent nanogel thermometer **1**, which is superior to other candidate thermometers[4−8] in terms of biocompatibility (i.e., size,[4,5] sensitivity,[6] and solubility[7]) and negligible interactions with cellular components.[8] Intracellular temperature variations associated with biological processes can be monitored with a temperature resolution of better than 0.5 °C using **1**.

Figure 1A shows a schematic diagram of the fluorescent nanogel thermometer **1**. The fluorescence switching of **1** is based on a strategy we previously established:[7a] the thermoresponsive polyNIPAM unit[9] was combined with a water-sensitive fluorophore (i.e., DBD-AA units[10] in this case). In addition, two arrangements were made to **1** in view of its need to function in intracellular environments. The first was gelation at the nanometer scale by an emulsion polymerization technique using a cross-linker (MBAM).[7b] The inclusion of fluorescent units in a nanogel can remove undesirable fluorescence enhancement/quenching due to chemical interactions between cellular components and the fluorophores. The second was the unique enrichment of ionic sulfate groups by using an extraordinary quantity of initiator ammonium persulfate in the preparation of **1** (i.e., the ammonium persulfate/NIPAM molar ratio was 0.28, while that in common procedures is 0.01−0.046).[7b,11] It is striking that conventional nanogels[7b] could not be applied in intracellular thermometry because of precipitation in the culture medium. In the present study, the highly hydrophilic surface created by the sulfate groups protected **1** from precipitation at high ionic strength and from localization on the cytoplasmic membrane.

The performance of **1**[12,13] in electrolytes was assessed using a spectrofluorometer. Figure 1B indicates the fluorescence response of **1** to the change in medium temperature at different ionic strengths. Potassium chloride was used as the ion source to mimic intracellular conditions, as K^+ is the most abundant ion in the cytoplasm (~139 mM).[14] As shown in Figure 1B, fluorescence enhancement of **1** with increasing temperature was observed in all measurements. As the KCl concentration increased from 0 to 100 mM, the response curve became sharper, producing a larger

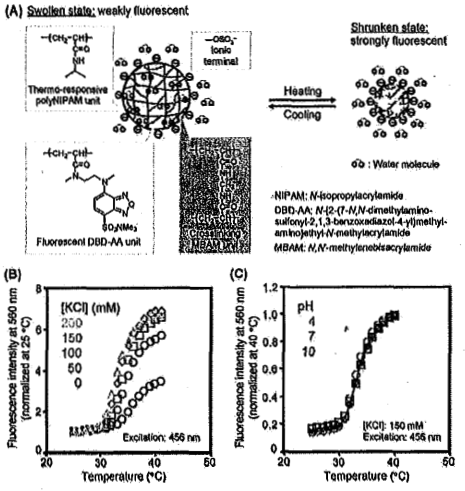

Figure 1. Fluorescent nanogel thermometer **1**. (A) Schematic diagram and chemical structures of the components. At a lower temperature, **1** swells by absorbing water into its interior, where the water-sensitive DBD-AA units are quenched by the neighboring water molecules. When heated, **1** shrinks with the release of water molecules, resulting in fluorescence from the DBD-AA units. (B) Fluorescence responses to temperature variation in water and in KCl solutions. (C) Insensitivity to pH variation. HCl and KOH were used for the pH adjustments. The fluorescence quantum yield was 0.37 at 40 °C.

fluorescence enhancement upon heating. In contrast, an almost identical response to the temperature variation was obtained when the KCl concentration was in the range 100−200 mM. This feature is desirable because the total ion concentration in the cytoplasm is equivalent to 150 mM.[14] The fluorescence response of **1** was independent of environmental pH, as indicated in Figure 1C. This is also advantageous because local pH in living cells is affected by neighboring structures and can easily vary by as much as one unit.[15] Furthermore, the performance of **1** was not even affected by a surrounding protein (e.g., bovine serum albumin; see Figure S4 in the Supporting Information). All of these results imply that **1** has a high capacity for accurate intracellular thermometry.

In this study on intracellular thermometry, COS7 cells were adopted as the subject of **1**. Highly hydrophilic **1** could easily be introduced into the cytoplasm by a microinjection technique without precipitation. Figure 2A shows representative phase-contrast and fluorescence images of living COS7 cells containing **1**. During the experiment, photobleaching and leaking of **1** were not problematic.[16] As shown in Figure 2A, **1** emitted fluorescence as dots at higher temperatures. These images show that **1** was dispersed within the cytoplasm but did not move to the nucleus. Figure 2B (left axis) indicates the calibration curve for intracellular thermometry with **1** (the relationship between total fluorescence intensity of **1** within a single COS7 cell and temperature). The total fluorescence intensity was obtained from fluorescence images by summing the fluorescence intensities of all the pixels within a single

[†] Graduate School of Pharmaceutical Sciences, The University of Tokyo.
[‡] The Tokyo Metropolitan Institute of Medical Science.
[§] Center for NanoBio Integration, The University of Tokyo.

10.1021/ja807714j CCC: $40.75

The subtle business of model reduction for stochastic chemical kinetics

Dan T. Gillespie,[1,a)] Yang Cao,[2] Kevin R. Sanft,[3] and Linda R. Petzold[3]
[1]*Dan T. Gillespie Consulting, 30504 Cordoba Place, Castaic, California 91384, USA*
[2]*Department of Computer Science, Virginia Tech, Blacksburg, Virginia 24061, USA*
[3]*Department of Computer Science, University of California Santa Barbara, Santa Barbara, California 93106, USA*

(Received 14 July 2008; accepted 28 December 2008; published online 10 February 2009)

This paper addresses the problem of simplifying chemical reaction networks by adroitly reducing the number of reaction channels and chemical species. The analysis adopts a discrete-stochastic point of view and focuses on the model reaction set $S_1 \rightleftharpoons S_2 \rightarrow S_3$, whose simplicity allows all the mathematics to be done exactly. The advantages and disadvantages of replacing this reaction set with a single S_3-producing reaction are analyzed quantitatively using novel criteria for measuring simulation accuracy and simulation efficiency. It is shown that in all cases in which such a model reduction can be accomplished accurately and with a significant gain in simulation efficiency, a procedure called the slow-scale stochastic simulation algorithm provides a robust and theoretically transparent way of implementing the reduction. © *2009 American Institute of Physics.* [DOI: 10.1063/1.3072704]

I. INTRODUCTION

Biochemical systems typically contain networks of many chemical reaction channels involving many molecular species. This circumstance encourages attempts to construct simpler but equivalent "reduced" reaction networks. A well known example of such a reduction is the Michaelis–Menten abridgment of the enzyme-substrate reactions,[1,2] which has been the subject of many refinements over the years[3,4] and which continues to play an important role in biochemistry today.[5]

Typically, an abridgment replaces the given reaction network with a network that involves fewer reaction channels and fewer chemical species. Perhaps the simplest reaction set that presents the opportunity for doing that, one that has several features in common with the enzyme-substrate reactions but is mathematically more tractable, is

$$S_1 \underset{c_2}{\overset{c_1}{\rightleftarrows}} S_2 \overset{c_3}{\rightarrow} S_3, \tag{1}$$

where we assume that c_1 and c_3 are both nonzero. It is tempting to cut to the chase and replace this set of three three-species reactions with one two-species reaction, such as

$$S_1 \overset{c}{\rightarrow} S_3, \tag{2}$$

where the reaction constant c is given some "suitable" value. Our focus in this paper will be to determine the conditions under which it is advisable to make such a replacement and to show how the replacement should be implemented. Of course, if a modeler deliberately chooses to model the production of S_3 molecules from S_1 molecules by reaction (2) instead of by reactions (1), then this issue is moot. But we are assuming here that the modeler believes that reactions (1) really describe what is going on physically, and therefore wants any abridgement of Eq. (1), such as reaction (2), to mimic the salient effects of reactions (1) with reasonable accuracy. A modeler might choose to use reaction (2) instead of reactions (1) because the values of the rate constants c_1, c_2, and c_3 in Eq. (1) are not all known. But choosing an appropriate value for c in Eq. (2) inevitably makes assumptions about those three rate constants; thus, it might be better to use Eq. (1) with those assumptions made explicitly and openly, since that would not only preserve the topology of reactions (1) but also make it easy to incorporate later new information about the unknown rate constants.

The most obvious advantage in replacing reactions (1) with a single S_3-producing reaction like Eq. (2) is the reduction in the numbers of reactions and species that we have to contend with. Another advantage might be speeding up the numerical simulation of reactions (1). By simulation we mean here *stochastic* simulation, since stochasticity often plays a role in cellular systems. But there are two potential drawbacks to such a reduction: First, as will be elaborated on below, this is always an approximation, since it is simply not possible for any single reaction to exactly mimic reactions (1) in all respects. Second, if we want to have the option of embedding reactions (1) in a larger network of reactions, some of which may involve species that get removed in the model reduction, as S_2 has in Eq. (2), then it may be impossible to simulate those other reactions when using the reduced model.

In this paper, we will address these matters in detail for reaction set (1). We will begin by presenting some novel perspectives on simulation *efficiency* and simulation *accuracy*. We will show that these new perspectives imply that a one-reaction abridgment of Eq. (1) will be advisable in some circumstances, but not in others. We will then show that, in all cases where a model reduction can be done accurately and with a significant gain in stochastic simulation efficiency,

a)Author to whom correspondence should be addressed. Electronic mail: gillespiedt@mailaps.org.

Molecular Microbiology (2009) 71(5), 1071–1087 ■

doi:10.1111/j.1365-2958.2008.06572.x
First published online 3 February 2009

Bacterial toxin YafQ is an endoribonuclease that associates with the ribosome and blocks translation elongation through sequence-specific and frame-dependent mRNA cleavage

Meredith H. Prysak,[1†] Christopher J. Mozdzierz,[1†] Angela M. Cook,[1] Ling Zhu,[2] Yonglong Zhang,[2] Masayori Inouye[2] and Nancy A. Woychik[1*]
Departments of [1]Molecular Genetics, Microbiology and Immunology, [2]Biochemistry, UMDNJ-Robert Wood Johnson Medical School, 675 Hoes Lane, Piscataway, NJ 08854, USA.

Summary

Toxin–antitoxin (TA) systems on the chromosomes of free-living bacteria appear to facilitate cell survival during intervals of stress by inducing a state of reversible growth arrest. However, upon prolonged stress, TA toxin action leads to cell death. They have been implicated in several clinically important phenomena – bacterial persistence during antibiotic treatment, biofilm formation and bacterial pathogenesis – and serve as attractive new antibiotic targets for pathogens. We determined the mode of action of the YafQ toxin of the DinJ–YafQ TA system. YafQ expression resulted in inhibition of translation, but not transcription or replication. Purified YafQ exhibited robust ribonuclease activity *in vitro* that was specifically blocked by the addition of DinJ. However, YafQ associated with ribosomes *in vivo* and facilitated rapid mRNA degradation near the 5′ end via cleavage at AAA lysine codons followed by a G or A. YafQ(H87Q) mutants lost toxicity and cleavage activity but retained ribosome association. Finally, LexA bound to the *dinJ–yafQ* palindrome and triggered module transcription after DNA damage. YafQ function is distinct from other TA toxins: it associates with the ribosome through the 50S subunit and mediates sequence-specific and frame-dependent mRNA cleavage at $^{5'}$AAA – G/A$^{3'}$ sequences leading to rapid decay possibly facilitated by the mRNA degradosome.

Accepted 3 December, 2008. *For correspondence. E-mail nancy.woychik@umdnj.edu; Tel. (+1) 732 235 4534; Fax (+1) 732 235 5223. †These two authors contributed equally to this work.

Introduction

Toxin–antitoxin (TA) systems/modules (also referred to as addiction or suicide modules) were first identified on plasmids due to their ability to induce post-segregational killing, because the cell becomes dependent on the presence of the TA-harbouring plasmid for survival (Gerdes *et al.*, 1986). However, these TA systems are also present on the chromosomes of free-living bacteria. Chromosomal TA modules typically comprise an autoregulated operon minimally encoding both a labile antitoxin and a more stable toxic protein (Gerdes *et al.*, 2005). All characterized chromosomal TA toxins facilitate inhibition of cell growth by targeting essential cell processes such as replication and translation. This inhibition appears to be an adaptation that facilitates stress survival. TA toxin-mediated growth arrest is reversible up to a 'point of no return', beyond which cell death occurs (Pedersen *et al.*, 2002). The function of the antitoxin, in contrast, is to prevent toxin activity during normal growth and enable finely tuned control of TA module toxicity during relatively short periods of environmental stress (Gerdes *et al.*, 2005).

There are five confirmed chromosomal TA loci in *Escherichia coli* K-12 cells: *relBE*, *yefM–yoeB*, *mazEF*, *chpBI-BK* and *hipBA* (Gerdes *et al.*, 2005). The toxins MazF and ChpBK are sequence-specific endoribonucleases that target free mRNA (independent of the ribosome) for degradation, thus indirectly perturbing translation (Christensen *et al.*, 2003; Zhang *et al.*, 2003; 2005a,b; Munoz-Gomez *et al.*, 2004). The RelE toxin also perturbs translation, but does so through interaction with the ribosome by preferentially targeting stop codons in a sequence-specific manner, with a preference for UAG (Christensen and Gerdes, 2003; Christensen *et al.*, 2001; Pedersen *et al.*, 2003). Although the *hipBA* TA system is poorly understood and its mechanism of toxicity is unknown, it appears to be a kinase whose action contributes to the formation of bacterial persisters upon antibiotic treatment (Keren *et al.*, 2004; Correia *et al.*, 2006; Korch and Hill, 2006). A sixth TA locus, *dinJ–yafQ*, has been recently identified (Motiejunaite *et al.*, 2007). The intracellular targets and precise mechanism of toxicity of YoeB, HipA and YafQ have not been identified.

Vol 457|29 January 2009|doi:10.1038/nature07568

LETTERS

Enterotoxigenic *Escherichia coli* EtpA mediates adhesion between flagella and host cells

Koushik Roy[1], George M. Hilliard[2], David J. Hamilton[3], Jiwen Luo[1], Marguerite M. Ostmann[4] & James M. Fleckenstein[1,2,5]

Adhesion to epithelial cells[1] and flagella-mediated motility are critical virulence traits for many Gram-negative pathogens, including enterotoxigenic *Escherichia coli* (ETEC)[2], a major cause of diarrhoea in travellers and children in developing countries[3,4]. Many flagellated pathogens export putative adhesins belonging to the two-partner secretion (TPS) family[5]. However, the actual function of these adhesins remains largely undefined. Here we demonstrate that EtpA, a TPS exoprotein adhesin of enterotoxigenic *E. coli*[6], mimics and interacts with highly conserved regions of flagellin, the major subunit of flagella, and that these interactions are critical for adherence and intestinal colonization. Although conserved regions of flagellin are mostly buried in the flagellar shaft[7], our results suggest that they are at least transiently exposed at the tips of flagella where they capture EtpA adhesin molecules for presentation to eukaryotic receptors. Similarity of EtpA to molecules encoded by other motile pathogens suggests a potential common pattern for bacterial adhesion, whereas participation of conserved regions of flagellin in adherence has implications for development of vaccines for Gram-negative pathogens.

ETEC cause diarrhoea by delivery of heat-labile and/or heat-stable enterotoxins to the small intestine, a process that requires critical fimbrial bacterial adhesins known as colonization factors[8,9]. These essential proteinaceous finger-like projections are central to ETEC vaccines currently in development[10]. Generally, adhesion to intestinal epithelium by diarrhoeagenic *E. coli* is a very complex process that may involve several structures including flagella[11]. The role of flagella in ETEC pathogenesis has not been sufficiently explored[12]. Flagella are complex cylindrical structures assembled from approximately 20,000 flagellin (FliC) molecules that travel down the nascent flagellar cylinder to the distal tip where they are directed by cap proteins (FliD)[13] into the growing flagellum. Flagellin has several major domains: the central domain projects on the surface of the flagellar shaft, accounting for antigenic variation used in *E. coli* 'H' serotyping; conserved amino- and carboxy-regions interact with adjacent subunits, facing the inaccessible shaft core[7].

Efficient adherence of ETEC to intestinal cells required both intact flagella and *etpA*; however, flagella-dependent adherence was independent of serotype, as complementation of a *fliC* ($H11^-$) mutant with *fliC* (H48) restored both motility and adherence (Fig. 1a). Likewise, antibody generated against (H48) full-length flagellin inhibited adherence of ETEC (H11) (Supplementary Fig. 1a) in contrast to antibody against serotype-dependent regions of flagellin (Supplementary Fig. 1b). Similarly, anti-EtpA antibodies inhibited adherence by EtpA-producing ETEC of multiple (H11, H12 and H16) serotypes whereas amounts of endogenous (Supplementary Fig. 1c) or exogenously added EtpA (Supplementary Fig. 1d) paralleled the adherence phenotype.

Recombinant EtpA labelled (Supplementary Fig. 2a) and bound specifically to the surface of intestinal cells, whereas antibodies against EtpA prevented this interaction (Fig. 1b). Interestingly, labelled EtpA localized to mucin-producing regions of the small intestine (Supplementary Fig. 2b), suggesting that EtpA could promote ETEC interaction with intestinal mucosal surfaces.

Theoretically, EtpA must maintain contact with ETEC to promote adherence. Attempts to purify recombinant EtpA from *E. coli*[6] were confounded by co-isolation of another protein (≈50 kilodaltons) despite attempted separation by column chromatography (Supplementary Fig. 3a), suggesting a potential protein–protein interaction[14]. Matrix-assisted laser desorption/ionization–time of flight (MALDI–TOF) definitively identified the co-purified protein as *E. coli* K-12 flagellin (H48, the same serotype as the recombinant used in the expression) (Supplementary Fig. 3b). Application of this purification strategy to ETEC strain H10407 (serotype H11) supernatants

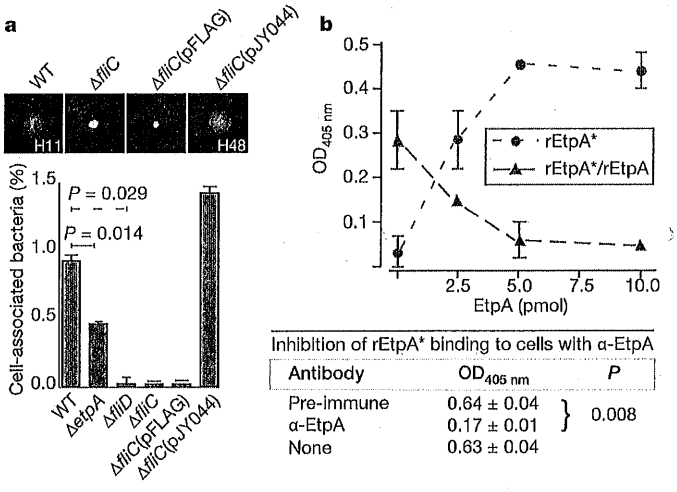

Inhibition of rEtpA* binding to cells with α-EtpA

Antibody	$OD_{405\,nm}$	P
Pre-immune	0.64 ± 0.04	0.008
α-EtpA	0.17 ± 0.01	
None	0.63 ± 0.04	

Figure 1 | EtpA and flagella contribute to ETEC adhesion. a, Efficient ETEC adherence requires production of EtpA and intact flagella, and is not dependent on flagellar serotype. WT, wild-type ETEC stain H10407. Complementation of the *fliC* ($H11^-$) isogenic deletion strain with pJY044 expressing *fliC* gene from MG1655 (*E. coli* K-12, flagellar serotype H48) restored motility and adherence phenotypes. *P* values (Mann–Whitney) generated by a one-tailed test (*etpA* mutant and wild type); others were two-tailed tests (mean ± s.d. for $n = 4$ replicates). **b,** EtpA binds specifically to target cells. Binding of purified biotinylated rEtpA (rEtpA*) to target Caco-2 epithelial cells was inhibited by unlabelled protein (mean values ($n = 3$) ± s.e.m.). Table below the graph demonstrates inhibition of EtpA* binding with EtpA antisera (mean values ($n = 3$) ± s.e.m.; $P = 0.0076$: unpaired *t*-test with Welch's correction).

[1]Department of Medicine, [2]Department of Molecular Sciences, [3]Department of Comparative Medicine, University of Tennessee Health Science Center, 956 Court Avenue, Memphis, Tennessee 38163, Tennessee, USA. [4]Research Service, [5]Medicine Service, Veterans Affairs Medical Center, 1030 Jefferson Avenue, Memphis, Tennessee 38104, USA.

ARTICLES

Life without a wall or division machine in *Bacillus subtilis*

M. Leaver[1], P. Domínguez-Cuevas[1], J. M. Coxhead[2], R. A. Daniel[1] & J. Errington[1]

The cell wall is an essential structure for virtually all bacteria, forming a tough outer shell that protects the cell from damage and osmotic lysis. It is the target of our best antibiotics. L-form strains are wall-deficient derivatives of common bacteria that have been studied for decades. However, they are difficult to generate and typically require growth for many generations on osmotically protective media with antibiotics or enzymes that kill walled forms. Despite their potential importance for understanding antibiotic resistance and pathogenesis, little is known about their basic cell biology or their means of propagation. We have developed a controllable system for generating L-forms in the highly tractable model bacterium *Bacillus subtilis*. Here, using genome sequencing, we identify a single point mutation that predisposes cells to grow without a wall. We show that propagation of L-forms does not require the normal FtsZ-dependent division machine but occurs by a remarkable extrusion-resolution mechanism. This novel form of propagation provides insights into how early forms of cellular life may have proliferated.

Binary fission is a widely conserved mechanism required for the proliferation of almost all cells. In bacteria, the central protein in cytokinesis is the bacterial tubulin homologue, FtsZ (filamentous temperature sensitive protein Z), which forms a ring (the Z-ring) to which other proteins are recruited[1]. The division machine then constricts in parallel with synthesis of a cross wall that matures into the new polar caps of the daughter cells[2] (Supplementary Fig. 1a). The machine includes enzymes called penicillin-binding proteins, which synthesize peptidoglycan, the major component of the wall[3] (Supplementary Fig. 1b). L-form bacteria[4,5] can proliferate but are thought not to have any wall; they offer an interesting model for investigating the details of Z-ring function[6], particularly whether constriction of the Z-ring requires wall synthesis.

A rapid method for generating L-forms

Existing L-form bacteria are difficult to manipulate[7], and modern genetic tools such as inducible promoters and green fluorescent protein (GFP) fusions have not been used in them. We therefore developed an approach to reproducibly generate stable *B. subtilis* L-forms.

We used strain M96 in which expression of the *murE* operon, which encodes several enzymes essential for the synthesis of the precursor of peptidoglycan[8], is controlled by the xylose inducible promoter P_{xyl}. In the presence of inducer, both the growth rate and the shape of this strain were normal (Fig. 1a–c). In the absence of inducer, cell growth was arrested and cells bulged and lysed (Fig. 1a, d). As previous work has shown that many shape mutants can be rescued by high concentrations of Mg^{2+} or osmoprotectants[9–12], we tested whether these conditions could restore growth to the MurE depletion strain. In the presence of high concentrations of Mg^{2+}, the growth of this strain was restored to a limited extent (Fig. 1a). Phase contrast microscopy of cells incubated in medium containing Mg^{2+} and sucrose revealed that lysis was reduced, and large, amorphous cells accumulated (Fig. 1e) that were similar in appearance to classically derived[7,13,14] and antibiotic induced L-forms[6]. These cells appeared to have little or no wall: when squashed between a microscope slide and a cover slip they packed together in a tessellated pattern, showing not only that they had lost their shape but also the rigidity of their envelope (Fig. 1f).

Unfortunately, these cells did not undergo sustained proliferation and the cultures were rapidly overrun with rod-shaped cells (Fig. 1g, arrowhead) presumably derived by spontaneous mutations in *xylR* or P_{xyl} that resulted in constitutive expression of *murE* in the absence of inducer. By introducing a second copy of the *xylR* repressor gene and selection with high concentrations of penicillin G (PenG, an antibiotic that inhibits cell wall synthesis by inactivating penicillin-binding proteins), occasional colonies of pure L-form-like cells were obtained, which could be propagated indefinitely (Methods). The frequency at which L-form-like colonies were generated was lower than the rate of formation of xylose resistant rod-shaped mutants, which presumably arose by mutation of the P_{xyl} promoter or double *xylR* mutants. It therefore seems likely that one or more secondary mutations are needed to produce cells that can proliferate in this L-form-like state.

A strain generated by this method (Bs115 sup21) had many of the properties of L-forms made by classical methods (Fig. 1h, Supplementary Results and Discussion)[7,15]. Importantly, strain Bs115 sup21 was about 1,000 times more resistant to PenG than the wild-type strain (Supplementary Fig. 2), consistent with the idea that L-forms do not make peptidoglycan (PenG probably has non-specific toxic effects at very high concentrations). Strain Bs115 sup21 did not require PenG to grow in the L-form state and, in the absence of PenG and presence of *murE* inducer (xylose), only reverted to rod shape at low frequency. This suggests that at least one of the putative secondary mutations that it had acquired prevents it from making cell wall.

A mutation that predisposes for L-form proliferation

The frequency with which L-forms arose suggested that one or two mutations were needed to generate L-forms. To test this, we performed shotgun sequencing[16] of the complete genome of a freshly derived L-form strain (Bs115 sup23). Approximately 700 polymorphisms were identified by comparison of the sequence to that published in the SubtiList database[17]. Only four of these were also found to be different

[1]Institute for Cell and Molecular Biosciences, Newcastle University, Framlington Place, Newcastle Upon Tyne NE2 4HH, UK. [2]Institute for Human Genetics, Newcastle University, International Centre for Life, Central Parkway, Newcastle Upon Tyne NE1 3BZ, UK.

Photoactivatable mCherry for high-resolution two-color fluorescence microscopy

Fedor V Subach[1–3], George H Patterson[2,3], Suliana Manley[2], Jennifer M Gillette[2], Jennifer Lippincott-Schwartz[2] & Vladislav V Verkhusha[1]

The reliance of modern microscopy techniques on photoactivatable fluorescent proteins prompted development of mCherry variants that are initially dark but become red fluorescent after violet-light irradiation. Using ensemble and single-molecule characteristics as selection criteria, we developed PAmCherry1 with excitation/emission maxima at 564/595 nm. Compared to other monomeric red photoactivatable proteins, it has faster maturation, better pH stability, faster photoactivation, higher photoactivation contrast and better photostability. Lack of green fluorescence and single-molecule behavior make monomeric PAmCherry1 a preferred tag for two-color diffraction-limited photoactivation imaging and for super-resolution techniques such as one- and two-color photoactivated localization microscopy (PALM). We performed PALM imaging using PAmCherry1-tagged transferrin receptor expressed alone or with photoactivatable GFP–tagged clathrin light chain. Pair correlation and cluster analyses of the resulting PALM images identified ≤200 nm clusters of transferrin receptor and clathrin light chain at ≤25 nm resolution and confirmed the utility of PAmCherry1 as an intracellular probe.

Genetically encoded 'photoactivatable' fluorescent proteins (PAFPs) make up a small category of fluorescent proteins[1], but are beginning to find uses far and above those of 'normal' fluorescent proteins[2]. With initially little or no fluorescence within their associated spectral detection window, photoactivatable proteins can be switched on by irradiation with violet light. Thus they are useful for spatially pulse-labeling subpopulations of molecules in cells in complement to photobleaching applications and can provide other useful features such as a high contrast over background in the photoactivated region and circumvention of fluorescence contributions from newly synthesized, nonactivated PAFPs. PAFPs and photoswitchable dyes also provide probes necessary for high-resolution optical techniques, such as photoactivated localization microscopy (PALM)[3], fluorescence photoactivated localization microscopy (FPALM)[4], stochastic reconstruction microscopy (STORM)[5], PALM with independent running acquisition (PALMIRA)[6] and stroboscopic PALM (SPALM)[7].

Of particular interest for PALM is the development of monomeric red PAFPs[8]. Several current variants can be activated into a red-emitting protein, but these have limitations for both live-cell confocal imaging and for high-resolution localization techniques. The obligate tetrameric state of red Kaede[9], KFP1 (ref. 10) and EosFP[11] frequently causes abnormal localization and function of the tagged proteins. Available monomeric red PAFPs such as Dendra[12], monomeric EosFP (mEosFP) or tandem dimeric EosFP (tdEosFP)[11] undergo the photoconversion from a green form to a red form, which complicates two-color photoactivation experiments with green PAGFP[13], PSCFP[14] or Dronpa[15]. It is also often difficult to achieve in cells a complete green-to-red photoconversion, which results in a detectable residual amount of the green species of these PAFPs. The available PAmRFP1 (ref. 8) switches from a nonfluorescent to a red fluorescent protein, but lacks the photon yields required for PALM applications. Reversibly photoswitchable fluorescent proteins rsCherry and rsCherryRev could be used in two-color experiments with green PAFPs, but have low brightness in their 'on' state, high background fluorescence in their 'off' state and tend to rapidly relax to the dark state after being photoswitched[16].

Here we report several irreversibly photoactivatable derivatives of mCherry[17], named PAmCherry proteins, with excellent photoactivation contrast over background, advanced photostability and high single-molecule brightness compatible with PALM imaging.

RESULTS

Development of photoactivatable mCherry variants

We analyzed data on color transitions of red fluorescent proteins to the respective nonfluorescent chromoproteins that had been generated by mutagenesis[1] and identified the corresponding crucial amino acid positions on the basis of the mCherry structure[18]. Positions spatially close to the chromophore, such as 148, 165, 167 and 203 (numbering is in accordance with GFP alignment; **Supplementary Fig. 1** online), appear to be major molecular determinants of color[10,19]. We hypothesized that mutagenesis of

[1]Department of Anatomy and Structural Biology, and Gruss-Lipper Biophotonics Center, Albert Einstein College of Medicine, 1300 Morris Park Ave., Bronx, New York 10461, USA. [2]Section on Organelle Biology, Cell Biology and Metabolism Program, National Institute of Child Health and Human Development, National Institutes of Health, 9000 Rockville Pike, Bethesda, Maryland 20892, USA. [3]These authors contributed equally to this work. Correspondence should be addressed to V.V.V. (vverkhus@aecom.yu.edu).

RECEIVED 11 NOVEMBER 2008; ACCEPTED 22 DECEMBER 2008; PUBLISHED ONLINE 25 JANUARY 2009; DOI:10.1038/NMETH.1298

A bright and photostable photoconvertible fluorescent protein

Sean A McKinney[1], Christopher S Murphy[2], Kristin L Hazelwood[2], Michael W Davidson[2] & Loren L Looger[1]

Photoconvertible fluorescent proteins are potential tools for investigating dynamic processes in living cells and for emerging super-resolution microscopy techniques. Unfortunately, most probes in this class are hampered by oligomerization, small photon budgets or poor photostability. Here we report an EosFP variant that functions well in a broad range of protein fusions for dynamic investigations, exhibits high photostability and preserves the ~10-nm localization precision of its parent.

The development of super-resolution imaging techniques has revolutionized the study of cellular ultrastructure with light microscopy. Photoactivated localization microscopy (PALM[1], PALMIRA[2] and FPALM[3]), reversible saturable optical fluorescence transitions (RESOLFT)[4], stochastic optical reconstruction microscopy (STORM)[5] and related methodologies, including dual-color[6], live-cell[3] and three-dimensional high-resolution imaging[7], are among the innovations that have allowed modest fluorescence microscopes to reach far beyond the traditional diffraction limit. These techniques share two critical enabling technologies: highly efficient detectors and fluorescent probes that photoswitch or photoconvert. Such probes allow the detection of single molecules over the background for high-precision localization and the repetitive excitation and selective quenching of subdiffraction annuli[4].

Fluorescent probes can be targeted to biological structures using either labeled antibodies or directly fused fluorescent proteins. Immunological fluorescence has the advantage of a larger probe palette from which to choose, including organic dyes. The number of photons obtainable per activation cycle, or photon budget, dictates the precision with which each fluorescent molecule is localized and, together with labeling density and background level, determines a probe's resolving power. Organic dyes, including Cy5 and Cy7, typically feature localization precisions approaching a lower limit of 4 nm[5]. However, the harsh conditions required for immunological fluorescence are undesirable. Furthermore, antibodies are limited in labeling density, often produce high nonspecific background, are seldom useful for live-cell imaging and can artificially inflate feature size by virtue of their own nontrivial dimensions[5].

For high-resolution applications that must overcome such problems, fluorescent protein fusions are currently the optimal solution. Unfortunately, the existing monomeric photoactivatable fluorescent proteins (PaFPs) suffer from smaller photon budgets than synthetic dyes, leading to a substantial loss in localization precision. The green-to-red photoconverting fluorescent proteins, Kaede and EosFP[1], yield precisions almost as good as organic dyes, but exist in solution as tetrameric complexes, hampering their use as fusion partners. Tandem dimer and monomeric versions of EosFP[8,9] (tdEos and mEos, respectively) have been engineered, but tdEos still does not localize accurately in fusions to many standard targets, including tubulin, histones, intermediate filaments and gap junctions (**Supplementary Methods** and **Supplementary Fig. 1** online), and mEos does not mature at 37 °C and can only be successfully used at 30 °C, at which most mammalian cells may exhibit metabolic artifacts. We developed mEos2, an mEosFP variant that folds efficiently at 37 °C and successfully labels targets that are intolerant of fusion to fluorescent protein dimers and tandem dimers. mEos2 preserves the localization precision of tdEos (~10 nm in one dimension) and serves as a traditional green-to-red optical highlighter with maturation kinetics, acid sensitivity, photostability and brightness comparable or superior to Dendra2 (ref. 10), the only other monomeric highlighter in its class.

We used side-chain grafting to stabilize mEos (wild-type EosFP with V123T and T158H). EosFP is homologous to the green reversibly photoactivatable protein Dronpa[11], which is bright, monomeric and matures well at 37 °C. Using protein structural alignment, we selected 20 positions for mutagenesis (**Supplementary Table 1** online) and found that three mutations (N11K, E70K and H74N) rescued fluorescence at 37 °C in bacterial colonies. mEos2, containing these three mutations and the serendipitous mutation H121Y, was a functional green-to-red photoconvertible fluorescent protein at 37 °C (**Supplementary Fig. 2** online). Modeling details are available in **Supplementary Methods**.

Purified mEos2 exhibited spectral properties, brightness, pK_a, photoconversion, contrast and maturation properties nearly identical to those of the earlier EosFP, dimeric EosFP (dEos; T158H) and tdEos (**Table 1** and **Supplementary Figs. 3–6** online). To examine oligomeric character, we used three techniques: gel filtration, homo–fluorescence resonance energy transfer (FRET)[12] and hetero-FRET (**Supplementary Figs. 7** and **8** online). Results suggested that mEos2 exhibited more dimeric character than its parent, but subsequent mutagenesis to remove this character proved detrimental in other ways (**Supplementary Fig. 9** online).

[1]Howard Hughes Medical Institute, Janelia Farm Research Campus, 19700 Helix Drive, Ashburn, Virginia 20147, USA. [2]National High Magnetic Field Laboratory and Department of Biological Science, The Florida State University, 1800 E. Paul Dirac Dr., Tallahassee, Florida 32310, USA. Correspondence should be addressed to L.L.L. (loogerl@janelia.hhmi.org) or M.W.D. (davidson@magnet.fsu.edu).

RECEIVED 31 OCTOBER 2008; ACCEPTED 15 DECEMBER 2008; PUBLISHED ONLINE 25 JANUARY 2009; DOI:10.1038/NMETH.1296

Noisy signaling through promoter logic gates

Moritz Gerstung,[1,2,*] Jens Timmer,[2,3] and Christian Fleck[2,4,†]
[1]*Department of Biosystems Science and Engineering, ETH Zurich, Mattenstrasse 26, 4058 Basel, Switzerland*
[2]*Institute of Physics, University of Freiburg, Hermann-Herder-Strasse 3a, 79104 Freiburg, Germany*
[3]*Freiburg Institute for Advanced Studies, Alberstrasse 19, 79104 Freiburg, Germany*
[4]*Center for Biological Systems Analysis, University of Freiburg, Habsburgerstrasse 49, 79104 Freiburg, Germany*
(Received 24 November 2007; revised manuscript received 24 October 2008; published 29 January 2009)

We study the influence of noisy transcription factor signals on cis-regulatory promoter elements. These elements process the probability of binary binding events analogous to computer logic gates. At equilibrium, this probability is given by the so-called input function. We show that transcription factor noise causes deviations from the equilibrium value due to the nonlinearity of the input function. For a single binding site, the correction is always negative resulting in an occupancy below the mean-field level. Yet for more complex promoters it depends on the correlation of the transcription factor signals and the geometry of the input function. We present explicit solutions for the basic types of AND and OR gates. The correction size varies among these different types of gates and signal types, mainly being larger in AND gates and for correlated fluctuations. In all cases we find excellent agreement between the analytical results and numerical simulations. We also study the *E. coli* Lac operon as an example of an AND NOR gate. We present a consistent mathematical method that allows one to separate different sources of noise and quantifies their effect on promoter occupation. A surprising result of our analysis is that Poissonian molecular fluctuations, in contrast to external fluctuations, do no contribute to the correction.

DOI: 10.1103/PhysRevE.79.011923 PACS number(s): 87.18.−h, 87.16.Yc

INTRODUCTION

Life is a phenomenon emerging from the subtle interplay of physical processes on a molecular scale. Nowadays, these processes are directly observable in single molecule experiments. This opens the door for bottom-up approaches to understand cellular function such as genetic regulation. In this fundamental biological process transcription factors (TFs) bind in response to environmental or cellular signals to specific DNA regions, the promoter, thereby triggering or inhibiting the expression of genes. If multiple TFs bind to distinct sites, thus integrating multiple signals, the promoter comprises a *cis*-regulatory module controlling gene expression through the Boolean combination of bound TFs [1,2]. The input-output behavior attributed to the transcriptional logic gate has been measured for various genes [3–6] at constant inducer levels. Because many TFs are present in low copy numbers per cell, however, the regulatory processes are inevitably stochastic.

Although there has been intense theoretical [7–14] and experimental work [15–23] on fluctuations arising from gene expression to explain cell-to-cell variations, little focus has been on the effect of such fluctuations on TF binding [24,25]. A common framework for quantifying molecular fluctuations in biochemical reactions are master equations [26]. These have been successfully used for the analysis of gene expression noise by various authors [8–10,27]. The inherent nonlinearity arising from the bimolecular TF-promoter interaction, however, impedes the analysis of the binding reaction with master equations substantially because moment-closure schemes fail. Therefore previous investigations on TF-promoter binding either used rate equations [28] or thermodynamic equilibrium models [1,29,30]. When concerning noise in genetic networks, several authors have used mean-field approximations [8,10,19] which are equivalent to a linearization of the system. Although these works have provided groundbreaking insights into the propagation of noise in genetic cascades, a systematic analysis of this nonlinear stochastic system is missing so far. This paper presents a detailed analysis of a TF-promoter interaction finding and quantifying noise-induced corrections due to the nonlinearity of the reactions. For a single binding site we find a negative correction to the mean-field level, while for *cis*-regulatory modules the correction depends nontrivially on the geometry of the input function and the correlation of the TF signals.

SINGLE SITE

We start by studying a single site and then extend the model to *cis*-regulatory modules. The single-site model consists of two reaction steps: First, TFs are synthesized with constant rate Γ and degraded proportional to the total number of TFs, n, with first-order rate constant D. In principle, this could also be a reversible activation or dimerization reaction if the amount of inactive (or monomer) TFs can be considered as a reservoir. Second, active TFs reversibly bind to a single promoter site s at rate j^+n and, in turn, dissociate at rate j^-:

$$\emptyset \underset{Dn}{\overset{\Gamma}{\rightleftharpoons}} n \underset{j^-}{\overset{j^+n}{\rightleftharpoons}} sn. \tag{1}$$

This kinetic model has been proposed previously by Berg *et al.* [24]. The reaction scheme manifests in the corresponding master equation,

*moritz.gerstung@bsse.ethz.ch
†christian.fleck@fdm.uni-freiburg.de

Plasmid 61 (2009) 89–93

Contents lists available at ScienceDirect

Plasmid

journal homepage: www.elsevier.com/locate/yplas

Meeting Report

EMBO Conference on Replication and Segregation of Chromosomes, Geilo, Norway, June 16–20
Replication and segregation of chromosomes in the three domains of life: EMBO conference reports common grounds
Meeting Report

Mirit Aladjem [a,*], Dhruba K. Chattoraj [b,*]

[a] *Laboratories of Pharmacology, Center for Cancer Research, NCI, NIH, 37 Convent Drive, Bethesda, MD 20892-4260, USA*
[b] *Biochemistry and Molecular Biology, Center for Cancer Research, NCI, NIH, 37 Convent Drive, Bethesda, MD 20892-4260, USA*

ARTICLE INFO

Article history:
Received 8 October 2008
Revised 29 October 2008
Available online 24 December 2008

Communicated by Manuel Espinosa

Keywords:
Replication
Segregation
Chromosome

ABSTRACT

A meeting of the EMBO Conference Series on Replication and Segregation of Chromosomes was held in Geilo, Norway, 16–20 June, 2008, under a scenic backdrop of high mountains. The meeting focused on the mechanistic details of replication and segregation primarily from well-characterized systems. Because the same basic principles govern chromosome maintenance in all three domains of life, participants encountering parallel processes in distantly-related organisms were stimulated to interact. Another successful aspect of the meeting was the quality of the posters, several of which were chosen for platform presentation and two for special rewards. The organizers Kirsten Skarstad and Erik Boye deserve praise for their skillful organization of the meeting, the highlights of which are discussed below.

1. Initiation of chromosome replication

Studies on DnaA protein, the initiator of many bacterial replicons, the *Escherichia coli* chromosome included, were started some 40 years ago by Kohiyama and Jacob; they continue still. T. Katayama (Japan) reported a new protein, DiaA (DnaA initiator-associating factor) that, as a tetramer, interacts with multiple DnaA molecules bound to the replication origin (*oriC*) and helps it to unwind. The gene for DiaA was identified earlier, as the locus of mutations that suppress the lethal over-replication of dnaAcos mutants at the nonpermissive temperature. Thus, DiaA seems to play a facilitatory role in replication initiation at the stage of origin opening. K. Skarstad (Norway) reported a new role of DnaA in sequestration of hemimethylated DNA in vivo. Sequestration is mediated by the SeqA protein that binds to newly replicated hemimethylated DNA and protects it from remethylation. The duration of sequestration is believed to depend on the density of adenine methylation (GATC) sites. The sequestration period is particularly long for *E. coli oriC*, where the density of GATC sites is 10 times higher than expected for a random DNA sequence. DnaA binding in the neighbourhood of GATC sites is now shown to extend the sequestration period. Since *oriC* has a high density of binding sites for both SeqA and DnaA, the contribution of DnaA to origin sequestration is likely to be significant. By keeping the origin in an inactive state, prolonging the sequestration period should help to prevent premature reinitiation. This is a new (and additional) role of DnaA in negative regulation of replication.

Sequestration aside, reinitiation is also delayed by the hydrolysis of DnaA-bound ATP to ADP. Since DnaA-ATP is the active form of the initiator and is also limiting for initiation, reactivation of inactive DnaA-ADP to DnaA-ATP is

* Corresponding authors.
E-mail addresses: aladjemm@mail.nih.gov (M. Aladjem), chattord@mail.nih.gov (D.K. Chattoraj).

doi:10.1016/j.plasmid.2008.10.003

Killing niche competitors by remote-control bacteriophage induction

Laura Selva[a], David Viana[a], Gili Regev-Yochay[b], Krzysztof Trzcinski[b], Juan Manuel Corpa[a], Íñigo Lasa[c], Richard P. Novick[d], and José R. Penadés[a,e,1]

[a]Universidad Cardenal Herrera-CEU, 46113 Moncada, Valencia, Spain; [b]Departments of Epidemiology and Immunology and Infectious Diseases, Harvard School of Public Health, Boston; [c]Instituto de Agrobiotecnología, CSIC-Universidad Pública de Navarra, 31006 Pamplona, Navarra, Spain; [d]Skirball Institute, New York University Medical Center, 540 First Avenue, New York, NY 10016; and [e]Centro de Investigación y Tecnología Animal, Instituto Valenciano de Investigaciones Agrarias (CITA-IVIA), Apdo. 187, 12.400 Segorbe, Castellón, Spain

Edited by Sankar Adhya, National Institutes of Health, Bethesda, MD, and approved December 3, 2008 (received for review September 26, 2008)

A surprising example of interspecies competition is the production by certain bacteria of hydrogen peroxide at concentrations that are lethal for others. A case in point is the displacement of *Staphylococcus aureus* by *Streptococcus pneumoniae* in the nasopharynx, which is of considerable clinical significance. How it is accomplished, however, has been a great mystery, because H_2O_2 is a very well known disinfectant whose lethality is largely due to the production of hyperoxides through the abiological Fenton reaction. In this report, we have solved the mystery by showing that H_2O_2 at the concentrations typically produced by pneumococci kills lysogenic but not nonlysogenic staphylococci by inducing the SOS response. The SOS response, a stress response to DNA damage, not only invokes DNA repair mechanisms but also induces resident prophages, and the resulting lysis is responsible for H_2O_2 lethality. Because the vast majority of *S. aureus* strains are lysogenic, the production of H_2O_2 is a very widely effective antistaphylococcal strategy. Pneumococci, however, which are also commonly lysogenic and undergo SOS induction in response to DNA-damaging agents such as mitomycin C, are not SOS-induced on exposure to H_2O_2. This is apparently because they are resistant to the DNA-damaging effects of the Fenton reaction. The production of an SOS-inducing signal to activate prophages in neighboring organisms is thus a rather unique competitive strategy, which we suggest may be in widespread use for bacterial interference. However, this strategy has as a by-product the release of active phage, which can potentially spread mobile genetic elements carrying virulence genes.

hydrogen peroxide | SOS response | *Staphylococcus aureus* | *Streptococcus pneumoniae* | bacterial interference

The interactions among bacteria living communally are highly complex and extremely interesting—illuminating, as they do, a long-ignored but nevertheless critical aspect of microbial biology. One can readily envision interactions such as direct competition for scarce nutrients, mutual cooperation for the conversion of substrates to utilizable metabolites, "borrowing" of quorum-sensing signals, DNA transfer, biofilm formation and maintenance, and interference or inhibition mediated by antibacterial products, including bacteriocins, antibiotics, and low-molecular-weight toxic compounds such as H_2O_2 (1). In this article, we consider a specific case of H_2O_2-mediated bacterial interference, that between pneumococci and *Staphylococcus aureus*, which, although well documented, occurs by an entirely unknown mechanism.

Several epidemiological studies have shown a negative association between carriage of *Streptococcus pneumoniae* and *S. aureus* (2, 3), raising public health concern that mass pneumococcal vaccination may cause an increase in *S. aureus* colonization and infection. As a case in point, it has been reported that children with recurrent otitis media vaccinated with the heptavalent pneumococcal vaccine had increased incidence of *S. aureus*-related acute otitis media and *S. aureus* colonization (3). Recent in vitro and in vivo studies have demonstrated that the interference between these 2 pathogens is related to hydrogen peroxide production by *S. pneumoniae*, which is bactericidal to *S. aureus* (4, 5). Similar observations have been reported for certain other pairs of bacteria (6). It is highly intriguing how the relatively low levels of hydrogen peroxide produced safely by some bacteria are bactericidal to others, despite the relative abundance of mechanisms protecting bacterial cells from oxidative damage, such as H_2O_2-inactivating enzymes and antioxidants (7) or DNA lesion repair systems (8).

Here, we shed light on the mechanism of interference between H_2O_2-producing bacteria and *S. aureus*. We present data supporting the idea that prophages may have a much greater role in bacterial ecology than has hitherto been suspected—namely, that killing of a target organism by "remote control" prophage induction may represent a major modality of directional bacterial interference. We show also that lysogenic staphylococci are much more sensitive to DNA-damaging antibiotics, such as fluoroquinolones, than nonlysogens, almost certainly for the same reason. Given the high prevalence of lysogeny, we can now predict that small, SOS-inducing molecules, produced in the environment at subinhibitory concentrations, may have strong selective value as effectors of directional interference.

Results

Hydrogen Peroxide Kills Only Lysogenic *S. aureus*. Several species of bacteria have H_2O_2-dependent bactericidal activity toward *S. aureus* (4, 9). However, the mechanism by which the relatively low levels of H_2O_2 produced by these organisms are bactericidal to *S. aureus* remains to be determined. One possibility is that H_2O_2 produced by one organism induces the SOS response in a competing (target) organism, lethally activating resident prophages in the latter. If so, staphylococcal lysogens but not nonlysogens should be sensitive to H_2O_2 and pneumococci should be insensitive, even though they are often or always lysogenic. Accordingly, we tested 8 strains of *S. aureus*, 6 lysogenic, 2 nonlysogenic (RN450 and V329), including a congenic pair in which one (RN10359) was an 80α lysogen of the other (RN450) and a strain producing the phage-carried PVL toxin (strain LUG855), lately implicated in serious staphylococcal infections [10; supporting information (SI) Table S1]. We used H_2O_2 at 0.5 mM, in the range ordinarily seen with pneumococcal cultures, and observed that all of the lysogenic strains were highly

Author contributions: J.R.P. designed research; L.S. and D.V. performed research; G.R.-Y., K.T., J.M.C., and I.L. contributed new reagents/analytic tools; L.S., D.V., I.L., R.P.N., and J.R.P. analyzed data; and G.R.-Y., K.T., R.P.N., and J.R.P. wrote the paper;

The authors declare no conflict of interest.

This article is a PNAS Direct Submission.

[1]To whom correspondence should be addressed. E-mail: jpenades@ivia.es.

This article contains supporting information online at www.pnas.org/cgi/content/full/0809600106/DCSupplemental.

www.pnas.org/cgi/doi/10.1073/pnas.0809600106

Optimization of gene expression by natural selection

Trevor Bedford[1] and Daniel L. Hartl[2]

Department of Organismic and Evolutionary Biology, Harvard University, 16 Divinity Avenue, Cambridge, MA 02138

Contributed by Daniel L. Hartl, November 25, 2008 (sent for review October 20, 2008)

It is generally assumed that stabilizing selection promoting a phenotypic optimum acts to shape variation in quantitative traits across individuals and species. Although gene expression represents an intensively studied molecular phenotype, the extent to which stabilizing selection limits divergence in gene expression remains contentious. In this study, we present a theoretical framework for the study of stabilizing and directional selection using data from between-species divergence of continuous traits. This framework, based upon Brownian motion, is analytically tractable and can be used in maximum-likelihood or Bayesian parameter estimation. We apply this model to gene-expression levels in 7 species of *Drosophila*, and find that gene-expression divergence is substantially curtailed by stabilizing selection. However, we estimate the selective effect, *s*, of gene-expression change to be very small, approximately equal to *Ns* for a change of one standard deviation, where *N* is the effective population size. These findings highlight the power of natural selection to shape phenotype, even when the fitness effects of mutations are in the nearly neutral range.

evolution | nearly neutral | Ornstein-Uhlenbeck | phenotypic optima

Abundant evidence indicates that natural selection is remarkably powerful in shaping nucleotide sequences (1, 2). Many tests of natural selection rely on a comparison between nonsynonymous sites, in which mutations affect protein sequence, and synonymous sites, in which mutations do not. Synonymous sites serve as a proxy for neutral sites, enabling the effects of selection to be distinguished from background mutational and demographic patterns. Although changes in gene expression are hypothesized to play a major role in adaptation (3, 4), changes in expression cannot be so easily partitioned into neutral and selected categories. Thus, methods derived to analyze selection in coding sequences cannot be readily applied to gene-expression data. In part because of this ambiguity, general forces acting on gene-expression divergence have remained unclear. At this point, there exists considerable debate over the relative importance of selection and random drift in shaping gene-expression levels (5–8).

The benefits of optimal gene regulation seem in many ways obvious. In the simple case of metabolic enzymes, underexpression may slow metabolic flux, while over-expression may expose the cell to additional toxic misfolded proteins (9). At the morphological level, gene regulation can be tightly coupled to phenotype (10, 11). Genetic mutations whose effects cascade into morphological differences are expected to have especially large fitness impacts, and as such will be heavily influenced by natural selection. A straightforward example of selection on gene-expression level can be seen in ribosomal proteins, which contrary to the neutral prediction are found to be highly expressed across a variety of organisms (12).

In this article, we present a model of gene-expression divergence that explicitly distinguishes between the forces of random genetic drift and natural selection. This work is based upon prior models of phenotypic trait evolution (13, 14). Our population genetic model is fundamentally similar to the Brownian motion model used to describe the random movements of physical particles (15). In both cases, the system is impacted by numerous tiny perturbations, in Brownian motion caused by collision but in the evolutionary context caused by mutations that are fixed in an evolving population. Owing to the central limit theorem, the resulting state of the system can be accurately described as a normally distributed random variable. In the simplest case, the probability of fixation of a random mutation is assumed to be independent of the current state of the system, and thus movement is not favored in one direction over the other. This scenario corresponds to selective neutrality. However, a slightly more complex model, described by the Ornstein-Uhlenbeck (OU) process, assumes that perturbations are more likely to shift the system toward some optimal value than away from it (16). This model does well to capture the essence of natural selection; mutations that produce a phenotype closer to some optimum are favored over those that produce a phenotype farther away.

Here, we analyze gene-expression levels across 7 species of *Drosophila* using the framework provided by the OU model. In the analysis, we compare expression divergence between species with estimates of time since their divergence based on sequence data. The pattern at which divergence in gene-expression levels accumulates over time does much to reveal the underlying forces of selection and drift. Using only species-level data, we find that stabilizing selection plays a major role in limiting divergence of gene-expression level. We also quantify the degree of selection and drift for specific genes, which illuminates the relationship between changes in gene sequence and changes in gene expression. Finally, we reconstruct the fitness landscape of gene-expression level, and find that although natural selection is pervasive in shaping gene expression, the individual fitness effects of changes in gene expression are rather weak.

Modeling Expression Divergence

Analogy to Brownian Motion. Here we apply models of Brownian motion to describe the variance in gene-expression level between orthologous genes as a function of the time separating these orthologs (13, 14). Brownian motion, also known the Wiener process, represents one of simplest continuous-time, continuous-state stochastic processes. In a Brownian motion, the degree of stochastic change away from the current state is independent of both state and time. The increment that a Brownian motion makes over a time interval of length 1 is normally distributed with mean 0 and variance σ^2. The "volatility" parameter σ completely describes the Brownian motion and determines the rate at which a trait's value diffuses away from its current state. In an evolutionary context, σ describes that rate of "phenotypic drift" experienced by a gene. Our use of the term drift differs from the classic usage, wherein drift refers to a systematic trend in the evolution of a Brownian motion. Genes in which expres-

Author contributions: T.B. and D.L.H. designed research; T.B. performed research; T.B. contributed new reagents/analytic tools; T.B. and D.L.H. analyzed data; and T.B. and D.L.H. wrote the paper.

The authors declare no conflict of interest.

[1]To whom correspondence may be addressed at: Department of Ecology and Evolutionary Biology, University of Michigan, 2041 Kraus Natural Science Building, 830 North University, Ann Arbor, MI 48109. E-mail: bedfordt@umich.edu.

[2]To whom correspondence may be addressed. E-mail: dhartl@oeb.harvard.edu.

This article contains supporting information online at www.pnas.org/cgi/content/full/0812009106/DCSupplemental.

Electron microscopy of whole cells in liquid with nanometer resolution

N. de Jonge[a,b,1], D. B. Peckys[b,c], G. J. Kremers[a], and D. W. Piston[a]

[a]Department of Molecular Physiology and Biophysics, Vanderbilt University Medical Center, Nashville, TN 37232-0615; [b]Materials Science and Technology Division, Oak Ridge National Laboratory, Oak Ridge, TN 37831-6064; and [c]University of Tennessee, Knoxville, TN 37996-2200

Edited by Jennifer Lippincott-Schwartz, National Institutes of Health, Bethesda, MD, and approved December 12, 2008 (received for review September 25, 2008)

Single gold-tagged epidermal growth factor (EGF) molecules bound to cellular EGF receptors of fixed fibroblast cells were imaged in liquid with a scanning transmission electron microscope (STEM). The cells were placed in buffer solution in a microfluidic device with electron transparent windows inside the vacuum of the electron microscope. A spatial resolution of 4 nm and a pixel dwell time of 20 μs were obtained. The liquid layer was sufficiently thick to contain the cells with a thickness of 7 ± 1 μm. The experimental findings are consistent with a theoretical calculation. Liquid STEM is a unique approach for imaging single molecules in whole cells with significantly improved resolution and imaging speed over existing methods.

cellular imaging | molecular labels

Understanding cellular function at a molecular level requires imaging techniques capable of imaging whole cells with a resolution sufficient to image individually tagged proteins. Electron microscopy and X-ray diffraction are traditionally used to resolve the structures of individual proteins and to image proteins distributions in cells (1). Imaging with these techniques demands extensive sample preparation to obtain, e.g., proteins crystals, stained thin sections, or frozen samples. The cells are thus not in their native liquid state. Light microscopy is used to image protein distributions via fluorescent labels on fixed cells in liquid and in live cells to investigate cellular function (2). Superresolution techniques surpass the diffraction limit in optical microscopy (3–6), but despite recent advances, these methods are still restricted to spatial resolutions >10–20 nm. Further, their optimal performance requires extended imaging times, and significant data postprocessing. The speed can only be increased at the cost of resolution.

Here, we describe a direct technique for imaging whole cells in liquid that offers nanometer spatial resolution and a high imaging speed. The principle is explained in Fig. 1. The eukaryotic cells in liquid are placed in a microfluidic flow cell with a thickness of up to 10 μm contained between 2 ultrathin electron transparent windows. This flow cell is placed in the vacuum of a STEM, using a fluid specimen holder. The annular dark field (ADF) detector in the STEM is sensitive to scattered electrons, which are generated in proportion to the atomic number (Z) of the atoms in the specimen (7, 8), so-called Z contrast, where the contrast varies with $\approx Z^2$. It is thus possible to image specific high-Z atoms, such as gold, inside a thick (several micrometer) layer of low-Z material, such as water, protein, or the embedding medium of a thin section (9). We used this approach to raster image single gold-tagged epidermal growth factor (EGF) molecules bound to cellular EGF receptors on fibroblast cells with a spatial resolution of 4 nm and a pixel dwell time of 20 μs.

Results

COS7 fibroblast cells were labeled with 10-nm gold nanoparticles conjugated with epidermal growth factor (EGF-Au). The cells were grown, labeled, and fixed directly on the silicon nitride windows. Fig. 2*A* shows the edge of a cell that was incubated for 5 min with EGF-Au. Gold labels are visible as bright spots and the cellular material as light-gray matter over the dark gray background. Bright spots vary in size from 2 to 5 pixels. The broader spots are generally dimmer, thus suggesting that these spots represent labels that were not at the vertical position of the focus in the sample. The density of the gold labels at the edge of the cell is a factor of 10 larger than in the dark background region, indicating specific labeling. Individual labels are scattered over the cell apart from several clusters containing 2 or 3 labels and up to a maximum of 9 labels. Images were recorded at 11 different positions at cell edges and data were also recorded for two other flow cells, showing similar results (data not shown). The localization of the labels at the cell edges is consistent with EGF receptors dispersed along the cell surface after 5 min of label incubation (10). A fraction of 0.42 of the electron beam was scattered by an angle larger than 70 mrad into the ADF detector. The time needed to image Fig. 2*A* was 21 s for a 1,024 × 1,024 pixel image with a pixel dwell time of 20 μs.

To observe molecular rearrangements in the COS7 cells, the cells were incubated for 10 min with EGF-Au followed by additional 15-min incubation in buffer. Liquid STEM images of these cells are shown in Fig. 2*B*. Circular clusters of labeled EGF receptors are visible. Imaging of a second flow cell with cells treated with the same protocol provided a similar result (data not shown). Sharp-edged gold labels are visible in the cluster at arrow 1, whereas the labels in the cluster at arrow 2 appear blurred and cannot be distinguished as individual labels, indicating that cluster 2 is out of the vertical plane of focus. The observation of circular clusters of labels at different vertical positions in the cell indicates that the labels were internalized. Circular clusters were not found in cells that were fixed after 5 min of incubation, where labels occurred individually, or in small groups of 2 - 9 labels (see Fig. 2*A* and Figs. S1–S4). The clustering of the EGF receptors and internalization of the labels is consistent with the known behavior of EGF-activation of EGF receptors, which cluster as internalized endosomes upon receptor activation (10). These images showed less contrast of the gold labels than in Fig. 2*A*. The detector semiangle was increased to 94 mrad to optimize the visibility of the labels. In this case, a fraction of 0.37 of the electron beam was scattered into the detector.

After STEM imaging, the flow cell used for Fig. 2*A* was opened and inspected for the presence of liquid, which was verified visually. The sample was then dried in air and imaged in the STEM (Fig. 2*C*). The fraction of electrons scattered into

Author contributions: N.d.J., D.B.P., G.J.K., and D.W.P. designed research; N.d.J., D.B.P., and G.J.K. performed research; N.d.J., D.B.P., and G.J.K. analyzed data; and N.d.J. and D.W.P. wrote the paper.

The authors declare no conflict of interest.

This article is a PNAS Direct Submission.

[1]To whom correspondence should be addressed. E-mail: niels.de.jonge@vanderbilt.edu.

This article contains supporting information online at www.pnas.org/cgi/content/full/0809567106/DCSupplemental.

Elongation dynamics shape bursty transcription and translation

Maciej Dobrzyński[a] and Frank J. Bruggeman[a,b,1]

[a]Centrum Wiskunde & Informatica, Kruislaan 413, 1098 SJ, Amsterdam, The Netherlands; and [b]Netherlands Institute for Systems Biology, Kruislaan 318, 1098 SM, Amsterdam, The Netherlands

Edited by Peter G. Wolynes, University of California at San Diego, La Jolla, CA, and approved December 19, 2008 (received for review April 10, 2008)

Cells in isogenic populations may differ substantially in their molecular make up because of the stochastic nature of molecular processes. Stochastic bursts in process activity have a great potential for generating molecular noise. They are characterized by (short) periods of high process activity followed by (long) periods of process silence causing different cells to experience activity periods varying in size, duration, and timing. We present an analytically solvable model of bursts in molecular networks, originally developed for the analysis of telecommunication networks. We define general measures for model-independent characterization of bursts (burst size, significance, and duration) from stochastic time series. Inspired by the discovery of bursts in mRNA and protein production by others, we use those indices to investigate the role of stochastic motion of motor proteins along biopolymer chains in determining burst properties. Collisions between neighboring motor proteins can attenuate bursts introduced at the initiation site on the chain. Pausing of motor proteins can give rise to bursts. We investigate how these effects are modulated by the length of the biopolymer chain and the kinetic properties of motion. We discuss the consequences of those results for transcription and translation.

bursts | interrupted Poisson process | transcriptional pausing | waiting times

The stochasticity of molecular processes contributes to heterogeneity in populations of isogenic cells. Cellular heterogeneity is manifested by differences in the copy numbers of molecules and in the timing and duration of processes. Recent advances in single-cell measurement have facilitated the quantification of stochastic phenomena (1–4) (reviewed in refs. 5 and 6). Together with models and theory much insight has been obtained into the sources of noise and how particular network designs contribute to noise suppression and amplification (7–10).

Stochasticity of gene expression has been described by distributions of macromolecules in a population of cells (1, 2). Whether averaging over a population captures the entire spectrum of molecular fluctuations a particular cell experiences over one generation, depends on magnitudes and rates of fluctuations. If these are slow but high in amplitude, the required averaging duration may extend over a generation span (11). Then, a single cell may not even be able to reach protein states accessible to other members, thus rendering cell–cell protein level distributions uninformative with respect to behavior of genetic circuits (12). In such cases, waiting times for individual birth and death events need to be monitored to assess physiological constraints on a single-cell level. This stochastic nature of waiting times will be our focus. Little analytical theory has been developed to deal with this phenomenon despite its relevance for single-cell behavior.

The waiting times in a first-order process with rate constant k follow an exponential distribution; the mean waiting time between events and its standard deviation are equal to $1/k$. The waiting time for an event is no longer exponentially distributed if it is regulated by another process. This mechanism underlies bursts in synthetic activity. The interrupted Poisson process (IPP) was introduced to study bursts in queuing and telecommunication theory (13). In an IPP, a stochastic switch modulates a process with exponentially distributed waiting times. Depending on the time scale separation between the process and the switch, multiple timescales may appear in waiting times for production events.

Bursts have received ample attention in the biophysics literature (5, 10, 14–17). These studies tend to focus predominantly on the protein number distributions, but do not analyze the distributions for waiting times in much depth. We show that such statistics are relevant for burst characterization and the molecular mechanisms giving rise to bursts.

Bursts have been experimentally observed for synthesis of mRNA and protein (3, 4, 18–22). They are characterized by rapid productions of a number of mRNA or protein molecules during short time intervals. Periods of synthetic silence occur between bursts. Bursts may give rise to significant disturbances of cellular physiology depending on burst size and the duration of synthetic silence and activity. Even though the benefit of bursts needs to be analyzed further, they could be beneficial for cells living in rapidly fluctuating environments (23). Bursts may give rise to a bimodal distribution of protein expression across cell populations (24). Thereby, 2 subpopulations could emerge having different adaptive potentials.

We apply the analytical theory of IPPs to a molecular mechanism for bursts. To identify and characterize bursts we derive 3 new indices: burst size, duration, and significance. We demonstrate how motor protein trafficking along biopolymer chains (such as mRNA polymerase and DNA polymerase along DNA, ribosomes along mRNA, and cargo-carrying dynein along microtubuli) can generate bursts depending on the length of the biopolymer and stochasticity of initiation and motion. We show that motor proteins can generate bursts by pausing or by memory of initiation bursts.

Analytical Expression of the Waiting Time Distribution

In this section, we study a small network to gain insight into burst-generating mechanisms. This will allow us to derive general indices for the characterization of burst properties. These indices will be applied to characterize biological mechanisms.

The network consists of a source switching between an inactive *OFF* and an active *ON* state according to a Poisson process (Fig. 1*A*). *OFF* and *ON* periods are defined on the level of the switch (see refs. 15 and 17 for the discussion of mechanisms giving rise to genetic switches). In the active state, production of P, e.g., mRNA or protein, occurs at exponentially distributed intervals of length $\tau_{ini} = 1/k_{ini}$. The average *ON* period lasts for $\tau_{on} = 1/k_{sw}^{-}$. Production periods are interrupted by transitions to the *OFF* state. Each rate constant corresponds to the inverse of the mean first passage time for a complex kinetic mechanism. We assume that it follows an exponential waiting time distribution.

Author contributions: M.D. and F.J.B. designed research, performed research, and wrote the paper.

The authors declare no conflict of interest.

This article is a PNAS Direct Submission.

[1]To whom correspondence should be addressed. E-mail: frank.bruggeman@sysbio.nl.

This article contains supporting information online at www.pnas.org/cgi/content/full/0803507106/DCSupplemental.

1: Q Rev Biophys. 2008 May;41(2):103-32.

Bacterial flagellar motor.

Sowa Y, Berry RM.

Clarendon Laboratory, Department of Physics, University of Oxford, Oxford, UK.

The bacterial flagellar motor is a reversible rotary nano-machine, about 45 nm in diameter, embedded in the bacterial cell envelope. It is powered by the flux of H+ or Na+ ions across the cytoplasmic membrane driven by an electrochemical gradient, the proton-motive force or the sodium-motive force. Each motor rotates a helical filament at several hundreds of revolutions per second (hertz). In many species, the motor switches direction stochastically, with the switching rates controlled by a network of sensory and signalling proteins. The bacterial flagellar motor was confirmed as a rotary motor in the early 1970s, the first direct observation of the function of a single molecular motor. However, because of the large size and complexity of the motor, much remains to be discovered, in particular, the structural details of the torque-generating mechanism. This review outlines what has been learned about the structure and function of the motor using a combination of genetics, single-molecule and biophysical techniques, with a focus on recent results and single-molecule techniques.

PMID: 18812014 [PubMed - indexed for MEDLINE]

We found 1 article by title matching your search:

1: Q Rev Biophys. 2008 Nov;41(3-4):181-204.

Feasibility of imaging living cells at subnanometer resolutions by ultrafast X-ray diffraction.

Bergh M, Huldt G, Timneanu N, Maia FR, Hajdu J.

Laboratory of Molecular Biophysics, Institute of Cell and Molecular Biology, Uppsala University, Uppsala, Sweden.

Detailed structural investigations on living cells are problematic because existing structural methods cannot reach high resolutions on non-reproducible objects. Illumination with an ultrashort and extremely bright X-ray pulse can outrun key damage processes over a very short period. This can be exploited to extend the diffraction signal to the highest possible resolution in flash diffraction experiments. Here we present an analysis of the interaction of a very intense and very short X-ray pulse with a living cell, using a non-equilibrium population kinetics plasma code with radiation transfer. Each element in the evolving plasma is modeled by numerous states to monitor changes in the atomic populations as a function of pulse length, wavelength, and fluence. The model treats photoionization, impact ionization, Auger decay, recombination, and inverse bremsstrahlung by solving rate equations in a self-consistent manner and describes hydrodynamic expansion through the ion sound speed. The results show that subnanometer resolutions could be reached on micron-sized cells in a diffraction-limited geometry at wavelengths between 0.75 and 1.5 nm and at fluences of 1011-1012 photons mum-2 in less than 10 fs. Subnanometer resolutions could also be achieved with harder X-rays at higher fluences. We discuss experimental and computational strategies to obtain depth information about the object in flash diffraction experiments.

PMID: 19079804 [PubMed - in process]

ments of *IIL1* activity under elevated temperatures, is the basis of the *iil* phenotype in Bur-0 plants.

RNA blots revealed longer *IIL1* transcript isoforms of minor abundance in Bur-0, independent of growth temperature (Fig. 4D). PCR analyses showed that this isoform retained only the intron containing the triplet expansion (Fig. 4E). The relatively weak effects are consistent with reports that GAA repeats are more likely than UUC repeats to affect splicing in mammalian cells (*25*). However, because normal splicing is not completely restored in a spontaneous revertant with an intermediate repeat length (Fig. 4E), the splicing defects alone cannot explain the observed differences in RNA expression levels. Nevertheless, inefficient splicing might contribute to reduced expression of mature *IIL1* transcripts, along with transcriptional defects, epigenetic changes, and post-transcriptional silencing (*26–28*).

If long repeats tended to be detrimental, as in the *IIL1* case, one would expect that these are rare in the genome. Indeed, less than 1% of all triplet repeats in the reference *A. thaliana* genome have six or more copies (table S3), and there is no expressed gene with more than 41 copies (table S4). The Bur-0 allele of *IIL1* itself seems to be rare, because we did not find it among 96 other *A. thaliana* strains nor in *Arabidopsis lyrata* (figs. S8 and S9). Several strains had either more (up to 36) or fewer than the 23 repeats in the Col-0 reference genome, and two strains had lost the triplets (Fig. 4F). These observations confirm the dynamic nature of the *IIL1* triplet repeat. Copy number variability in normal individuals is common for triplet expansion disorders in humans and often underlies genetic anticipation (*5*, *6*).

The *A. thaliana* Bur-0 allele of *IIL1* presents a genetically tractable model for the study of triplet repeat expansion and contraction across multiple generations. The recovery of phenotypic revertants that had retained the expanded *IIL1* repeat highlights the potential of the *IIL1* triplet repeat for future studies. Some of the apparent second-site mutations might act downstream of *IIL1*, but others might ameliorate the effects of the triplet repeat expansion itself. In addition, our findings support the argument that simple sequence repeats could be associated with phenotypic variability of evolutionary significance (*1–3*).

References and Notes

1. E. Levdansky *et al.*, *Eukaryot. Cell* **6**, 1380 (2007).
2. T. P. Michael *et al.*, *PLoS One* **2**, e795 (2007).
3. K. J. Verstrepen, A. Jansen, F. Lewitter, G. R. Fink, *Nat. Genet.* **37**, 986 (2005).
4. J. W. Fondon 3rd, E. A. Hammock, A. J. Hannan, D. G. King, *Trends Neurosci.* **31**, 328 (2008).
5. H. T. Orr, H. Y. Zoghbi, *Annu. Rev. Neurosci.* **30**, 575 (2007).
6. C. E. Pearson, K. Nichol Edamura, J. D. Cleary, *Nat. Rev. Genet.* **6**, 729 (2005).
7. L. Y. Brown, S. A. Brown, *Trends Genet.* **20**, 51 (2004).
8. R. D. Wells, R. Dere, M. L. Hebert, M. Napierala, L. S. Son, *Nucleic Acids Res.* **33**, 3785 (2005).
9. M. H. Hoffmann, *J. Biogeography* **29**, 125 (2002).
10. Supporting tables, figures, and materials and methods are available as supporting material on *Science* Online.
11. S. I. Bidichandani, T. Ashizawa, P. I. Patel, *Am. J. Hum. Genet.* **62**, 111 (1998).
12. E. Grabczyk, K. Usdin, *Nucleic Acids Res.* **28**, 2815 (2000).
13. K. Ohshima, L. Montermini, R. D. Wells, M. Pandolfo, *J. Biol. Chem.* **273**, 14588 (1998).
14. R. D. Wells, *FASEB J.* **22**, 1625 (2008).
15. B. Zybailov *et al.*, *PLoS ONE* **3**, e1994 (2008).
16. G. B. Kohlhaw, *Microbiol. Mol. Biol. Rev.* **67**, 1 (2003).
17. T. Knill, S. Binder, personal communication.
18. R. Schwab, S. Ossowski, M. Riester, N. Warthmann, D. Weigel, *Plant Cell* **18**, 1121 (2006).
19. M. Simon *et al.*, *Genetics* **178**, 2253 (2008).
20. R. M. Clark *et al.*, *Hum. Genet.* **120**, 633 (2007).
21. I. De Biase *et al.*, *Genomics* **90**, 1 (2007).
22. R. Sharma *et al.*, *Hum. Mol. Genet.* **11**, 2175 (2002).
23. V. I. Hashem *et al.*, *Nucleic Acids Res.* **32**, 6334 (2004).
24. V. I. Hashem, R. R. Sinden, *Mutat. Res.* **508**, 107 (2002).
25. M. Baralle, T. Pastor, E. Bussani, F. Pagani, *Am. J. Hum. Genet.* **83**, 77 (2008).
26. S. Al-Mahdawi *et al.*, *Hum. Mol. Genet.* **17**, 735 (2008).
27. R. Frisch *et al.*, *Mol. Genet. Metab.* **74**, 281 (2001).
28. E. Greene, L. Mahishi, A. Entezam, D. Kumari, K. Usdin, *Nucleic Acids Res.* **35**, 3383 (2007).

29. We are very grateful to T. Knill and S. Binder for sharing unpublished information. We acknowledge experimental support from our colleagues at the Max Planck Institute and University of Queensland. We also thank them as well as J. Carrington and D. Tautz for critical reading of the manuscript, and the European *Arabidopsis* Stock Centre and the French National Institute for Agricultural Research (INRA) at Versailles for seeds. Supported by an EMBO (*European Molecular Biology Organization*) Long-Term Fellowship (S.B.), Marie Curie Research Training Network SY-STEM, European Research Area—Plant Genomics (ERA-PG) Deutsche Forschungsgemeinschaft ARelatives Consortium, European Union Sixth Framework Programme for Research and Technological Development Integrated Project (EU FP6 IP) Agronomics (LSHG-CT-2006-037704), a Leibniz Award (DFG), and the Max Planck Society (D.W.). GenBank accession numbers are FJ665284 to FJ665378.

Supporting Online Material

www.sciencemag.org/cgi/content/full/1164014/DC1
Materials and Methods
Figs. S1 to S9
Tables S1 to S4
References

31 July 2008; accepted 11 December 2008
Published online 15 January 2009;
10.1126/science.1164014
Include this information when citing this paper.

Stress-Inducible Regulation of Heat Shock Factor 1 by the Deacetylase SIRT1

Sandy D. Westerheide,[1*] Julius Anckar,[2*] Stanley M. Stevens Jr.,[3] Lea Sistonen,[2] Richard I. Morimoto[1†]

Heat shock factor 1 (HSF1) is essential for protecting cells from protein-damaging stress associated with misfolded proteins and regulates the insulin-signaling pathway and aging. Here, we show that human HSF1 is inducibly acetylated at a critical residue that negatively regulates DNA binding activity. Activation of the deacetylase and longevity factor SIRT1 prolonged HSF1 binding to the heat shock promoter Hsp70 by maintaining HSF1 in a deacetylated, DNA–binding competent state. Conversely, down-regulation of SIRT1 accelerated the attenuation of the heat shock response (HSR) and release of HSF1 from its cognate promoter elements. These results provide a mechanistic basis for the requirement of HSF1 in the regulation of life span and establish a role for SIRT1 in protein homeostasis and the HSR.

Transient activation of heat shock factor 1 (HSF1) by diverse environmental and physiological stress is a multistep process that involves constitutive expression of an inert HSF1 monomer, conversion of the monomer to a DNA–binding competent trimer, increased phosphorylation of HSF1 at serine residues, enhanced transcription, and attenuation of HSF1 DNA binding and transcriptional activity (*1*). HSF1 activates the transcription of a large number of genes that regulate protein homeostasis including the molecular chaperones heat shock proteins 70 and 90 (Hsp70 and Hsp90, respectively). These chaperones associate with HSF1 to initiate a negative-feedback loop and to inhibit HSF1 transcriptional activity (*2*). However, HSF1 is not released from its target promoter sites (*3*); this suggests that additional mechanisms must exist to complete the HSF1 cycle.

Stress resistance and metabolic state are intimately coupled to protein homeostasis and increased life span. In *Caenorhabditis elegans*, the protective effects of reduced insulin signaling require HSF1 and the FOXO transcription factor DAF-16 to prevent damage by protein misfolding and to promote longevity (*4*, *5*). The beneficial effects of low caloric intake are mediated by the sirtuin family member Sir2, a deacetylase that is dependent on nicotinamide adenine dinucleotide (oxidized form) (NAD) and that is under metabolic control (*6*). The mammalian Sir2 homolog SIRT1 regulates the transcription factor FOXO3 among

[1]Department of Biochemistry, Molecular Biology and Cell Biology, Rice Institute for Biomedical Research, Northwestern University, Evanston, IL, 60208, USA. [2]Department of Biology, Turku Centre for Biotechnology, Åbo Akademi University, FI-20520 Turku, Finland. [3]University of Florida, Protein Chemistry Core Facility, Interdisciplinary Center for Biotechnology Research, Gainesville, FL 32610, USA.

*These authors contributed equally to this work.
†To whom correspondence should be addressed. E-mail: r-morimoto@northwestern.edu

SYSTEMS BIOLOGY

Attractors and Democratic Dynamics

Cellular transcription networks are conceptualized as distributed control systems that regulate gene expression.

Yaneer Bar-Yam,[1] Dion Harmon,[1] Benjamin de Bivort[1,2]

The functional identity of a cell is largely determined by the regulated expression (transcription) of thousands of genes, so how it maintains a particular transcriptional state is of critical importance. Developmental biologists study how embryonic cells navigate a series of intermediate transcriptional states before settling into a final adult state; microbiologists identify the mechanisms by which transcription is altered by environmental perturbation; and oncologists seek to identify how cells switch from benign to cancerous. Consider two concepts of transcriptional regulation. In a "molecular autocracy," master genes respond to environmental or developmental stimuli by regulating thousands of genes, either directly or through other transcription factors. In a "molecular democracy," all genes exert a regulatory influence on all other genes, and phenotypic change (altered cell behavior) is brought about through the concerted action of thousands of genes. These scenarios are extreme and cells operate under a condition that is somewhere intermediate (see the figure) (*1*). But the choice of concept affects how regulation is studied.

The autocratic framework can be directly investigated by studies of individual molecular mechanisms and has been the starting point for discussions of biological processes. But a broader understanding of regulatory mechanisms is needed that incorporates essential features of both extreme views. The democratic framework relies on mutual regulation, which tends toward a self-consistent gene expression state that is stable in the face of fluctuations. In other words, this view has its roots in the conceptual understanding of stability and homeostasis of cell types (*2*, *3*). The democratic view has only recently gained empirical support, perhaps because its characterization involves studies of genome-wide dynamical processes.

A dynamic system with extensive mutual regulation tends to transition toward particular states, known as attractors, over time (often envisioned as valleys in a landscape). Background "noise" causes deviation in one cell over time, and among cells at one instant, but they recover. That there is an attractor state in the space of transcriptional states (*4*, *5*) supports the prediction of a democratic system. Chang *et al.* (*6*) recently identified transcriptional variability in clonally related mouse hematopoietic precursor cells, and separated the cells into several groups with expression differences in thousands (but still a minority) of genes. Over days, these cell group lineages converged to the same transcriptional state distribution. That is, the cell groups became indistinguishable, having the same average gene expression, as well as noise-induced variation, among individual cells. Such convergence is the signature of an attractor, in which many individual differences in transcription are insufficient to change the overall cell phenotype (a "controlling" majority of transcribed genes does not change) and mutual interactions among the genes cause trends toward specific mutually reinforcing states.

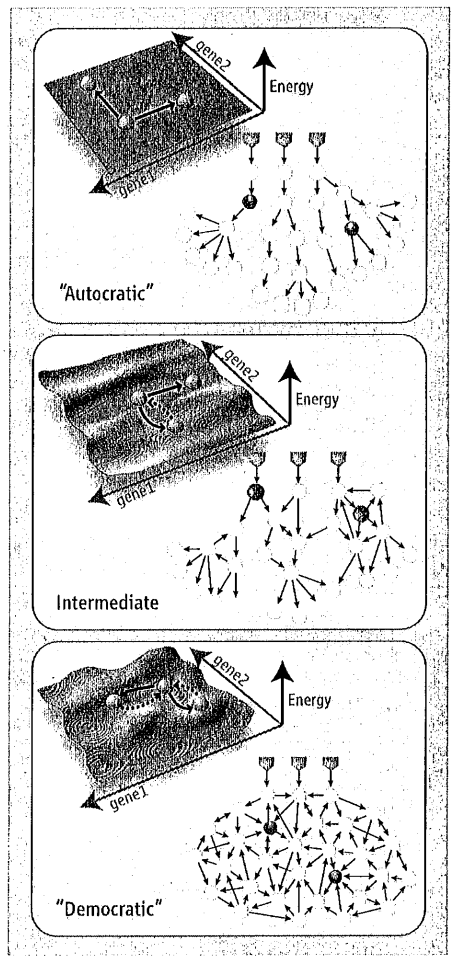

Transcription regulatory architecture. In autocratic regulatory networks (**top**), individual master regulator genes (pointed squares) are stimulated by external signals and control many other genes (circles). As shown by the energy landscape, the transcriptional states (spheres) may have no preferences (black arrows represent changes in expression of genes 1 and 2). In democratic networks (**bottom**), all genes act as mutual regulators. A few specific gene expression patterns become stable, shown as basins of attraction (cell types) in the landscape. Once a cell reaches one of these states, changing the expression of one gene is unlikely to switch the cell type (black arrows). Intermediate networks (**middle**) have mutual regulation, but certain genes (blue circle) are major controllers.

The attractor paradigm has practical implications: If distinct cell types (such as a precursor cell and a fully differentiated cell) correspond to distinct attractors, then there are multiple parallel ways to shift the transcriptional state from one attractor to another. Such families of trajectories are expected to engage multiple interconnected signaling pathways whose collective behavior (and outcome) is simple. In a limited way, this has been observed in the differentiation of immune cells (*4*) and stem cells (*7*). If the attractor picture is generically valid, it should be possible to create cocktails of large numbers of gene products that switch cells between different types. Any sufficiently large subset of gene products should be sufficient to cause the switch. Consider the number of gene expression levels that are needed to robustly characterize distinct cell types. An analysis (see fig. S1) of the transcriptional profiles of 79 human tissues and tumor cell types (*8*) reveals that about 200 highly variable gene expression values are sufficient to capture the relationships among the tissues and tumor cells, whereas fewer than 80 are not. By this measure, cocktails with a couple of hundred gene products chosen to mimic the differences between two cell types should generically cause transitions between them.

Still, paradoxically, Chang *et al.* (*6*) segregated cells according to the expression of a single gene, and showed that specific genes can

[1]New England Complex Systems Institute, 24 Mt. Auburn Street, Cambridge, MA 02138, USA. [2]Roland Institute at Harvard University, 100 Edwin Land Boulevard, Cambridge, MA 02139, USA. E-mail: yaneer@necsi.edu

Published by AAAS

CELL BIOLOGY

The Force Is with Us

Martin A. Schwartz

Through changes in protein conformation and interactions, cells sense and respond to forces at their point of attachment to extracellular matrix.

The ability of cells and tissues to respond to mechanical force is central to many aspects of biology. Areas relevant to human physiology and disease include development and maintenance of bone, blood vessels, and muscles; regulation of blood pressure; motility of cells; and regulation of cell proliferation (*1*). Mechanosensitive adhesions mediated by membrane proteins called integrins are believed to underlie a number of these behaviors (*2*). Forces applied either by the cells' own cytoskeleton or from external sources induce strengthening of these adhesions and trigger a variety of intracellular signals through these effects. Two papers in this issue, one by Friedland *et al.* on page 642 (*3*) and the other by del Rio *et al.* on page 638 (*4*), increase our understanding of the molecular basis for these phenomena.

Current models for mechanotransduction generally involve alterations in protein conformation by forces (*1*, *5*). Stretch-activated membrane channels, present in cells from all organisms that have been examined, undergo conformational transitions in response to changes in membrane tension. For cytoskeletal and extracellular matrix proteins that form linear polymers, tension is thought to cause partial or complete unfolding of domains, exposing new binding sites or other motifs. The extracellular matrix protein fibronectin is the best-studied example. Fibronectin requires tension to assemble into fibrils (*6*, *7*), and fluorescence resonance energy transfer measurements showed that fibronectin in fibrils is in an extended state (*8*). Stretching fibronectin exposes a cryptic binding site in the first type III domain, leading to associations between fibronectin proteins that promote fibril formation (*6*).

Integrins are one link in a connection that runs from extracellular matrix proteins such as fibronectin across the plasma membrane to the actin cytoskeleton. Integrins form this connection in part by binding the cytoskeletal protein talin, which binds actin directly, as well as by recruiting the cytoskeletal protein vinculin, which also binds actin (*9*). Because every component in this chain experiences tension, each one is in principle a potential mechanotransducer.

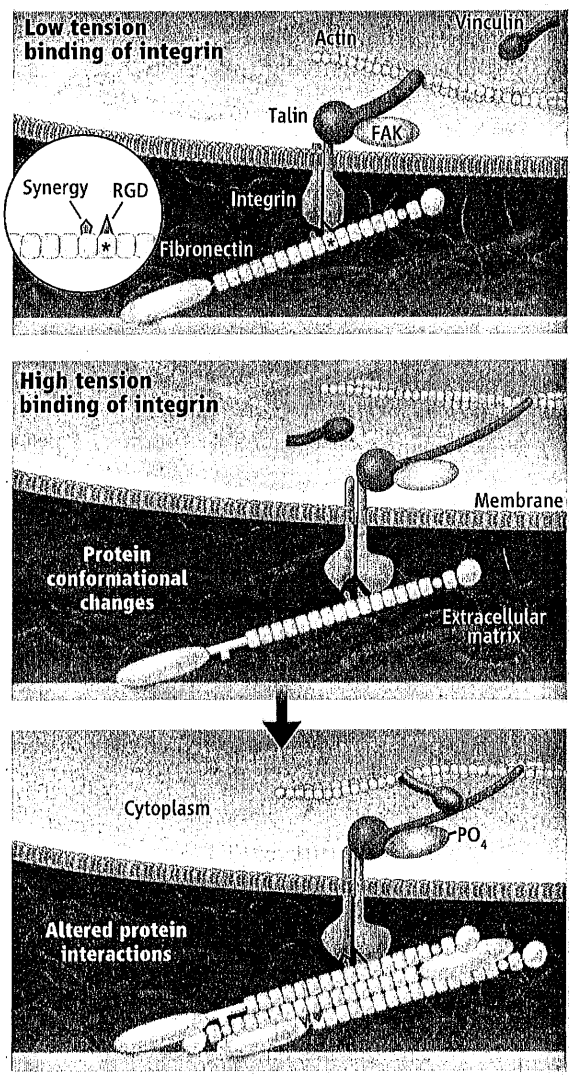

Force mechanics. At points of cell attachment to extracellular matrix, when tension is low, integrin $\alpha_5\beta_1$ binds to the RGD sequence in fibronectin. The cytoplasmic domain of integrin $\alpha_5\beta_1$ is associated with talin, but most vinculin binding sites on talin are inaccessible. Increased tension triggers conformational changes in the integrin, talin, and fibronectin. These alterations reveal new vinculin binding sites in talin, enhance the affinity of $\alpha_5\beta_1$ for the synergy site in fibronectin, and reveal new self-association sites in fibronectin. These changes lead to increased vinculin binding to talin, tighter binding of the integrin to fibronectin, increased fibronectin matrix assembly, and activation of FAK. These events may also promote increased clustering of integrins.

The best-defined response of integrin-dependent cell adhesions to tension is reinforcement of the adhesions to resist the applied force (*2*). These responses occur over several time scales. Over tens of seconds, vinculin is recruited to small adhesions, most likely without recruitment of additional integrins (*10*). Over a few minutes, adhesions grow larger and lengthen in the direction of the applied force (*11*), which appears to involve recruitment of additional integrins. Indeed, application of force by stretching elastic substrata triggers conversion of unoccupied, low-affinity integrins to a high-affinity state, which induces new binding to the extracellular matrix (*12*). These reinforcement mechanisms may also mediate changes in downstream signaling. Indeed, the activity of focal adhesion kinase (FAK), a tyrosine kinase that transduces multiple signals from integrins, requires actin- and myosin-dependent tension (*13*).

Friedland *et al.* provide evidence that the major fibronectin-binding integrin, $\alpha_5\beta_1$, undergoes a force-dependent conformational transition. This conclusion is based on the ability of integrin $\alpha_5\beta_1$ to be chemically cross-linked to fibronectin. Force is required for conversion of the bond from a non–cross-linkable to a cross-linkable state, suggesting a change in proximity of key residues. Integrin $\alpha_5\beta_1$ binds to two sites in fibronectin: an Arg-Gly-Asp (RGD) sequence in the 10th type III repeat and a secondary (so-called) synergy site in the 9th repeat (*7*) (see the figure). Friedland *et al.* also show that conversion to the cross-linkable state requires the synergy site and that these events correlate with phosphorylation (thus, activation) of FAK. The picture that emerges from these results is that initial low-tension binding of integrin $\alpha_5\beta_1$ to fibronectin involves association of the integrin with the RGD sequence, which under force converts to a higher-strength, more readily cross-linked bond that involves the synergy site. Only this second conformation can activate FAK and transmit downstream signals.

Talin is the focus of the study by del Rio *et al.* It binds directly to the β_1 inte-

Departments of Microbiology, Cell Biology, and Biomedical Engineering, Cardiovascular Research Center and Mellon Urological Cancer Research Institute, University of Virginia, Charlottesville, VA 22908, USA. E-mail: maschwartz@virginia.edu

Published by AAAS

Dynamical Quorum Sensing and Synchronization in Large Populations of Chemical Oscillators

Annette F. Taylor,[1] Mark R. Tinsley,[2] Fang Wang,[2] Zhaoyang Huang,[2] Kenneth Showalter[2]*

Populations of certain unicellular organisms, such as suspensions of yeast in nutrient solutions, undergo transitions to coordinated activity with increasing cell density. The collective behavior is believed to arise through communication by chemical signaling via the extracellular solution. We studied large, heterogeneous populations of discrete chemical oscillators (~100,000) with well-defined kinetics to characterize two different types of density-dependent transitions to synchronized oscillatory behavior. For different chemical exchange rates between the oscillators and the surrounding solution, increasing oscillator density led to (i) the gradual synchronization of oscillatory activity, or (ii) the sudden "switching on" of synchronized oscillatory activity. We analyze the roles of oscillator density and exchange rate of signaling species in these transitions with a mathematical model of the interacting chemical oscillators.

From the periodic firing of neurons to the flashing of fireflies, the synchronization of rhythmic activity plays a vital role in the functioning of biological systems (*1–3*). The mechanisms by which single cells or whole organisms coordinate their activity continue to inspire research over a range of disciplines (*4–6*). Synchronization may occur by global coupling, where each oscillator is connected to every other oscillator through a common (mean) field. With this mechanism, mathematically formalized by Kuramoto (*7*), oscillators are regulated by the average activity of the population (the mean field) and a collective rhythm emerges above a critical coupling strength. A number of oscillatory systems are thought to synchronize by this mechanism (*8*, *9*), such as stirred suspensions of the cellular slime mold *Dictyostelium discoidium* (*10*), but it has been experimentally characterized only recently in a system of coupled electrochemical oscillators (*11*).

A distinctly different type of transition to synchronized oscillatory behavior has been observed in suspensions of yeast cells (*12*). The density-dependent transition, discovered by Aldridge and Pye (*13*) more than 30 years ago, recently has been studied in a stirred-flow reactor configuration (*14*). Relaxation experiments reveal that slightly below the critical cell density, the system is made up of a collection of quiescent cells rather than unsynchronized oscillatory cells, whereas slightly above the critical density, the cells oscillate in nearly complete synchrony (*12*). This type of transition is much like quorum-sensing transitions in bacteria populations, where each member of a population undergoes a sudden change in behavior with a supercritical increase in the concentration of a signaling molecule (autoinducer) in the extracellular solution (*15*). Many examples of quorum-sensing transitions have been found, such as the appearance of bioluminescence in populations of *Vibrio fischeri* (*16–18*) and biofilm formation in *Pseudomonas aeruginosa* (*19*).

We studied a population of chemical oscillators to characterize the transition to synchronization as a function of population density and transport rate of signaling species to the surrounding solution. We used porous catalytic particles (~100 μm in radius) that were suspended in a fixed volume of catalyst-free Belousov-Zhabotinsky (BZ) reaction mixture (*20*, *21*). The catalyst for the reaction, $Fe(phen)_3^{2+}$ (ferroin), is immobilized on the cation exchange particles (*22*, *23*). Reagents in the solution react with the ferroin to produce an activator, $HBrO_2$, which catalyzes its own production, and an inhibitor, Br^-, which inhibits autocatalysis. A catalyst-loaded particle changes from red to blue as ferroin is oxidized and $HBrO_2$ is produced. The oxidized metal catalyst reacts with solution reagents to regenerate the reduced form of the catalyst and Br^-. The cycle repeats when the inhibitor level falls sufficiently. Each catalyst-loaded particle has its own oscillatory period, on the order of 1 min (45 ± 13 s), which depends on the catalyst loading and the particle size. The period distribution (fig. S1) is obtained by monitoring the color change associated with the oxidation of the ferroin catalyst on each particle in unstirred solutions (*21*, *24*).

A sketch of the experimental setup is shown in Fig. 1. Both the activator $HBrO_2$ and inhibitor Br^- are exchanged between the catalyst particles and the surrounding solution, with the exchange rate depending on the stirring rate (*21*). The surrounding solution is monitored with a Pt electrode, where the potential increases with an increasing concentration of $HBrO_2$ relative to Br^-, and the oxidation state of the particles is monitored by high-speed video (*21*). The first time series in Fig. 1 illustrates the change in amplitude of the potential as the oscillator density is increased. The second time series shows the corresponding average intensity obtained from the mean of the individual particle intensities in each image (scaled by the average intensity of fully oxidized particles). When all particles are simultaneously oxidized, the scaled average intensity increases from 0 (all particles red) to 1 (all particles blue), and the value is less than 1 when a fraction of the population is oxidized. The coherence of the population can be seen in images of the stirred particles (Fig. 1).

We observed two distinct types of transitions to synchronous activity, depending on the stirring rate. One type occurs at low stirring rates, as

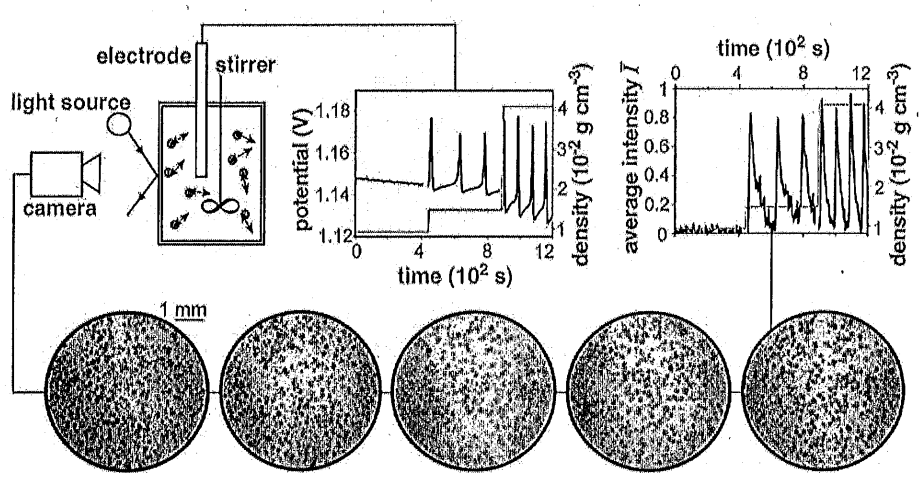

Fig. 1. Experimental setup (*21*). Catalytic microparticles are globally coupled by exchange of species with the surrounding catalyst-free BZ reaction solution. Electrochemical time series illustrates the change in oscillatory amplitude and period with increasing particle density (red line) for a stirring rate of 600 rpm. A typical series of images obtained during one oscillation is shown, from which the (normalized) average intensity of the particles is calculated as a function of time. The associated time series illustrates the change in oscillatory amplitude and period with increasing particle density (red line) for a stirring rate of 600 rpm. A density of 0.02 g cm^{-3} corresponds to ~1.3×10^4 particles cm^{-3}.

[1]School of Chemistry, University of Leeds, Leeds LS2 9JT, UK. [2]C. Eugene Bennett Department of Chemistry, West Virginia University, Morgantown, WV 26506, USA.

*To whom correspondence should be addressed. E-mail: kshowalt@wvu.edu